# Lactosylceramide contributes to mitochondrial dysfunction in diabetes

**Sergei A. Novgorodov,[1,*] Christopher L. Riley,[†] Jin Yu,[*] Jarryd A. Keffler,[*] Christopher J. Clarke,[§] An O. Van Laer,[†,**] Catalin F. Baicu,[†,**] Michael R. Zile,[†,**] and Tatyana I. Gudz[*,†]**

Departments of Neuroscience* and Medicine,** Medical University of South Carolina, Charleston, SC 29425; Ralph H. Johnson Veteran Affairs Medical Center,[†] Charleston, SC 29401; and Department of Medicine,[§] Stony Brook University, Stony Brook, NY 11794

**Abstract Sphingolipids have been implicated as key mediators of cell-stress responses and effectors of mitochondrial function. To investigate potential mechanisms underlying mitochondrial dysfunction, an important contributor to diabetic cardiomyopathy, we examined alterations of cardiac sphingolipid metabolism in a mouse with streptozotocin-induced type 1 diabetes. Diabetes increased expression of desaturase 1, (dihydro)ceramide synthase (CerS)2, serine palmitoyl transferase 1, and the rate of ceramide formation by mitochondria-resident CerSs, indicating an activation of ceramide biosynthesis. However, the lack of an increase in mitochondrial ceramide suggests concomitant upregulation of ceramide-metabolizing pathways. Elevated levels of lactosylceramide, one of the initial products in the formation of glycosphingolipids were accompanied with decreased respiration and calcium retention capacity (CRC) in mitochondria from diabetic heart tissue. In baseline mitochondria, lactosylceramide potently suppressed state 3 respiration and decreased CRC, suggesting lactosylceramide as the primary sphingolipid responsible for mitochondrial defects in diabetic hearts. Moreover, knocking down the neutral ceramidase (NCDase) resulted in an increase in lactosylceramide level, suggesting a crosstalk between glucosylceramide synthase- and NCDase-mediated ceramide utilization pathways. These data suggest the glycosphingolipid pathway of ceramide metabolism as a promising target to correct mitochondrial abnormalities associated with type 1 diabetes.—** Novgorodov, S. A., C. L. Riley, J. Yu, J. A. Keffler, C. J. Clarke, A. O. Van Laer, C. F. Baicu, M. R. Zile, and T. I. Gudz. **Lactosylceramide contributes to mitochondrial dysfunction in diabetes. *J. Lipid Res.* 2016.** 57: **546–562.**

**Supplementary key words** glycolipids • sphingolipids • calcium • heart • respiration • mitochondria

Compelling epidemiological and clinical data indicate that diabetes mellitus increases the risk for cardiac dysfunction and heart failure independently of other risk factors, such as coronary disease and hypertension. Lipotoxicity is an important contributor to cardiac dysfunction in both type 1 (1, 2) and type 2 (3–6) diabetes, which are characterized by excessive accumulation of triacylglycerols, long-chain acyl-CoAs, diacylglycerols, and ceramides in myocardium. Correlation of the increased ceramide level with development of diabetic cardiomyopathy has attracted special attention in recent years because of the well-documented ability of this sphingolipid to regulate a number of cell processes, including cell proliferation, growth arrest, differentiation and apoptosis, and the mediation of responses to stress stimuli.

Ceramide is a hub of sphingolipid metabolism (7, 8). The balance between ceramide-producing pathways and pathways that consume it dictates ceramide level in the cell. The de novo ceramide biosynthesis pathway, one of the major ceramide producing pathways, localizes in the endoplasmic reticulum (ER) and starts with the condensation of serine and palmitoyl-CoA producing 3-ketosphingonine, which, in turn, is rapidly converted to dihydrosphingosine. Subsequent acylation of dihydrosphingosine by a set of (dihydro)ceramide synthases (CerSs) gives rise to dihydroceramide. Finally, the removal of two hydrogens from the fatty acid chain of dihydroceramide by desaturase leads to the formation of ceramide. Other possible contributors to elevated ceramide level are: hydrolysis of SM catalyzed by SMases,

*This work was supported in part by the American Diabetes Association Innovation Award 7-12-IN-28 (S.A.N.), VA Merit Awards I01BX002991 (T.I.G.), I01CX000415-02 (M.R.Z.), I01BX000487-04 (M.R.Z.), and National Institutes of Health Grants RO1NS083544 (T.I.G.), R56HL123478 (M.R.Z.), and 1R01HL123478-01A1 (M.R.Z.). The Lipidomics Core Facility at the Medical University of South Carolina was in part supported by National Institutes of Health Grant P30 GM10333. The content is solely the responsibility of the authors and does not necessarily represent the official views of the National Institutes of Health.*

*Manuscript received 15 April 2015 and in revised form 16 February 2016.*

*Published, JLR Papers in Press, February 21, 2016*
*DOI 10.1194/jlr.M060061*

Abbreviations: CerS, ceramide synthase; CRC, calcium retention capacity; CSA, cyclosporin A; DNP, 2,4-dinitrophenol; EF, ejection fraction; ER, endoplasmic reticulum; FB1, fumonisin B1; IB, isolation buffer; IFM, interfibrillar mitochondria, LA, left atrial; LV, left ventricular; LVW, left ventricular weight; MAM, mitochondria-associated membranes; mPTP, mitochondrial permeability transition pore; NCDase, neutral ceramidase; ROS, reactive oxygen species; SPT, serine palmitoyl transferase; SSM, subsarcolemmal mitochondria; STZ, streptozotocin; SV, stroke volume; TMPD, *N,N,N′,N′*-tetramethyl-*p*-phenelenediamine; VDAC, voltage dependent anion channel.

[1] To whom correspondence should be addressed.
e-mail: novgoros@musc.edu

acylation of sphingosine in the salvage pathway, dephosphorylation of ceramide-1-phosphate, and catabolism of glycosphingolipids.

Ceramide levels are tightly controlled in the cells via rapid transformation into less harmful sphingolipids. The main pathway of ceramide utilization is its conversion to sphingosine and FFA catalyzed by ceramidases, which reside in mitochondria, plasma membrane, lysosomes, and Golgi compartments (neutral, acid, and alkaline ceramidases). Ceramide can also be channeled to the formation of complex glycosphingolipids. The first step in this pathway is catalyzed by glucosylceramide synthase with the formation of glucosylceramide. Subsequent formation of lactosylceramide and further gangliosides gives rise to a wide spectrum of biologically active molecules. Conversion to SM (SM synthase) and ceramide-1-phosphate (ceramide kinase) are other alternatives for ceramide utilization.

Mitochondria emerged as a novel specialized compartment of sphingolipid metabolism with their own subset of sphingolipid-generating and -degrading enzymes. Neutral ceramidase (NCDase) (9–11), a novel neutral SMase (12, 13), CerS (14), and sphingosine kinase 2 (10, 15), which convert sphingosine to sphingosine-1-phosphate, have been found associated with mitochondria. Mitochondria contain a variety of sphingolipid species and some of their effects on mitochondrial function are well-documented (16). For example, ceramide suppresses mitochondrial respiratory chain activity (17), potentiates insertion of Bax into the outer mitochondrial membrane (18), and, depending on the conditions, can accelerate or suppress the opening of the mitochondrial permeability transition pore (mPTP) (19–21) of the inner mitochondrial membrane. Similarly, sphingosine suppresses respiratory chain activity (10, 22, 23) and mPTP opening (23–25). Potentiation of mPTP opening by ganglioside GD3 (26, 27) and increased mitochondrial reactive oxygen species (ROS) production in the presence of lactosylceramide (28) have also been reported.

Altered mitochondrial substrate and energy metabolism, along with the increased propensity for mitochondria-mediated cell death are important contributors to the development of reduced cardiac efficiency in diabetic cardiomyopathy (6, 29–32). Mitochondrial dysfunction in type 1 diabetic heart tissue is the result of inhibition of the respiratory chain (33–35), oxidative stress (35, 36), and decreased resistance to $Ca^{2+}$- (37, 38) and oxidative stress-induced mPTP opening (39, 40).

The goal of this investigation was to determine the effect of type 1 diabetes, induced by streptozotocin (STZ), on cardiac mitochondrial sphingolipid makeup and identify the sphingolipids contributing to mitochondrial dysfunction. We evaluated two distinct mitochondrial subpopulations: subsarcolemmal mitochondria (SSM) and interfibrillar mitochondria (IFM), which differ with respect to their respiratory capacity, sensitivity to $Ca^{2+}$, and response to type 1 diabetic insult (41, 42). There were no substantial increases in ceramide level in both subpopulations in diabetic heart tissue, despite an upregulation of CerS2, serine palmitoyl transferase (SPT) 1, and desaturase 1 expression, indicative of activation of the de novo ceramide biosynthesis pathway. This suggests concert activation of ceramide-producing and ceramide-utilizing reactions. Indeed, NCDase-deficient mice display increased ceramide levels after induction of diabetes, suggesting NCDase-mediated ceramide hydrolysis as an important checkpoint in the control of mitochondrial ceramide. An activation of ceramide-consuming pathways gains additional support due to the substantial rise in lactosylceramide upon induction of diabetes in WT mice, which was further enhanced in NCDase-null mice, especially in IFM. Evaluation of the effects of exogenous lactosylceramide on baseline IFM revealed suppression of the respiratory chain and decreased calcium retention capacity (CRC). These studies suggest that type 1 diabetes does not induce ceramide accumulation in heart mitochondria, but rather increases ceramide flux, and that, not ceramide, but ceramide-derived glycosphingolipid lactosylceramide mediates the mitochondrial dysfunction.

## MATERIALS AND METHODS

### Animals and reagents

Male C57BL/6 mice were from The Jackson Laboratory (Sacramento, CA). NCDase KO mice were generated in the laboratory of Dr. Richard Proia (43) (National Institute of Diabetes and Digestive and Kidney Diseases, National Institutes of Health) and transferred to the animal facility of the Medical University of South Carolina. The mice were C57BL/6 background and were backcrossed for 10 additional generations with the same background at the Medical University of South Carolina. Experimental protocols were reviewed and approved by the Institutional Animal Care and Use Committee of the Medical University of South Carolina (Charleston, SC) and followed the National Institutes of Health guidelines for experimental animal use. Diabetes was induced in 8- to 9-week-old mice following the Low-Dose Streptozotocin Induction Protocol (Mouse) of the Diabetic Complications Consortium. Animals were fasted for 4 h prior to STZ injection. Injections (ip) were performed at 50 mg/kg body weight of STZ dissolved in sodium citrate buffer (pH 4.5) for five consecutive days. Plasma glucose levels were monitored with TRUEread blood glucose monitor (Nipro-Diagnostics, Fort Lauderdale, FL) and animals with glucose levels >300 mg/dl were considered diabetic. Control animals were given injections of citrate buffer. Alternatively, animals with diabetes induced by the similar protocol were obtained from the Jackson Laboratory. Five weeks postinjection animals were used for experimentation. TPCK-treated trypsin and soybean trypsin inhibitor were from Worthington Biochemical Corporation (Lakewood, NJ). According to manufacturer's specification, 1 mg inhibitor suppresses activity of 2.06 mg trypsin. The 17C-sphingosine, palmitoyl-CoA, arachidoyl-CoA, $C_{16:0}$-lactosylceramide, and $C_{16:0}$-glucosylceramide were from Avanti Polar Lipids (Alabaster, AL). All other chemicals were purchased from Sigma-Aldrich (St. Louis, MO).

### Antibodies

Antibodies against mitochondrial marker, voltage dependent anion channel (VDAC) (D73D12), and syntaxin 6 (Golgi marker) were supplied by Cell Signaling Technology (Danvers, MA). The

rabbit polyclonal anti-LAMP-2 (lysosomal marker), mouse monoclonal anti-α1 subunit of the $Na^+/K^+$ ATPase (plasma membrane marker), and the rabbit polyclonal anti-calnexin (ER marker) antibodies were purchased from Abcam (Cambridge, MA). Rabbit polyclonal anti-SPTLC1 antibody was purchased from Abcam. Goat polyclonal anti-SPTLC2 (C20), rabbit polyclonal anti-SPTLC3 (D-13), rabbit polyclonal anti-UGCG (H-300), and rabbit polyclonal anti-CerS2 antibodies were purchased from Santa Cruz Biotechnology, Inc. (Santa Cruz, CA). Rabbit polyclonal anti-NCDase antibody was raised by Bethyl Laboratories (Montgomery, TX) (10). Mouse monoclonal anti-β-actin antibody (AC-74) was purchased from Sigma-Aldrich. Secondary horseradish peroxidase-conjugated antibodies were supplied by Jackson ImmunoResearch Laboratories Inc. (West Grove, PA).

### Echocardiography

Mice underwent echocardiography to examine in vivo changes in cardiac function upon induction of diabetes using a 40 MHz mechanical scanning transducer (707B) and a Vevo 770 echocardiograph (VisualSonics, Toronto, Canada), as previously described (44). Left ventricular (LV) weight (LVW), LV ejection fraction (EF), stroke volume (SV), and left atrial (LA) dimension were measured using the American Society of Echocardiography criteria (45). LVW was normalized to body weight.

### Preparation of mitochondria from cardiac tissue

SSM and IFM were isolated according to Palmer, Tandler, and Hoppel (41) and King et al. (34) with some modifications. Hearts from eight to ten mice were minced and washed in isolation buffer (IB) consisting of 100 mM KCl, 50 mM MOPS, 1 mM EGTA, 5 mM $MgSO_4$, and 1 mM ATP (pH 7.4 adjusted by KOH). Minced tissue was diluted 1:10 (w/v) in IB and homogenized with a Polytron tissue processor (Brinkman Instruments, Westbury, NY) for 3 s at a rheostat setting of 6.5, and further homogenized with a motorized Potter-Elvejhem homogenizer by five strokes at 800 rpm. Homogenate was centrifuged at 600 *g* for 10 min. Supernatant was saved and the pellet was resuspended in IB. After repeated centrifugation at 600 *g* for 10 min, the supernatants were combined and the pellet was saved for isolation of IFM. SSM were pelleted from supernatant by centrifugation at 3,100 *g* for 10 min. To isolate IFM, pellet from the last centrifugation at 600 *g* was suspended in IB containing trypsin (5 mg/g wet weight) for 10 min at 4°C. Digestion was terminated by addition of an equal volume of IB containing soybean trypsin inhibitor (5 mg/g wet weight) and the suspension was centrifuged at 7,700 *g* for 10 min. Supernatant was discarded and myofibril pellet was resuspended in IB and spun down at 600 *g* for 10 min. Supernatant was saved and the procedure was repeated one more time. IFM were obtained from combined supernatants by centrifugation at 3,100 *g* for 10 min. To increase purification of SSM and IFM, pellets were resuspended in IB and spun down at 3,100 *g* for 10 min. This step was repeated one more time, however, mitochondria were resuspended in a buffer containing 100 mM KCl, 50 mM MOPS, and 0.5 mM EGTA (pH 7.4 adjusted by KOH). After final centrifugation, mitochondria were resuspended in the above mentioned buffer. Mitochondria had negligible contamination with the major cellular membrane compartments, as assessed by Western blot using antibodies against plasma membrane marker protein ($Na^+$,$K^+$-ATPase), lysosomes (LAMP-2), ER (calnexin), and Golgi marker (syntaxin 6) (**Fig. 1**). As expected, the outer mitochondrial membrane marker VDAC was enriched in the mitochondrial fractions as compared with homogenate.

### Protein determination

Mitochondrial protein concentration was quantified with a bicinchoninic acid assay kit (Pierce, Rockford, IL) using BSA as a standard.

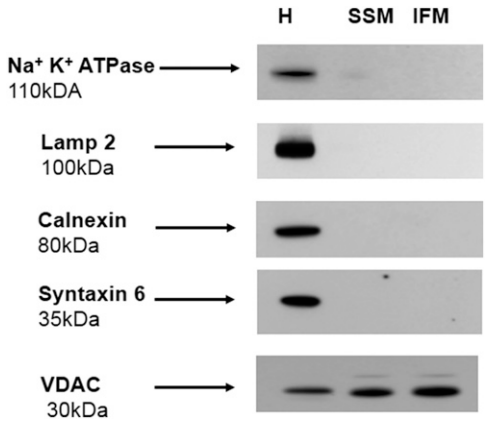


**Fig. 1.** Heart mitochondria display minimal contamination with other cellular membrane compartments. Western blots for $Na^+$,$K^+$-ATPase (plasma membrane marker), LAMP-2 (lysosomal marker), calnexin (ER marker), syntaxin 6 (Golgi marker), and VDAC (mitochondrial marker) were performed by loading equal amounts of 30 μg of homogenate (H), or mitochondrial (SSM or IFM) protein per lane, except VDAC, which was assessed using protein loading of 15 μg per lane. The blot is representative of three independent experiments.

### Measurement of mitochondrial permeabilization

Inner membrane permeabilization was assayed by measurements of the decrease in absorbance of mitochondrial suspension, indicative of mitochondrial swelling, at 520 nm using a Brinkmann PC 910 probe colorimeter and a fiber optic probe, as we described (20).

### CRC of mitochondria

The CRC of mitochondria was monitored using a $Ca^{2+}$-selective electrode (ThermoScientific/Orion, Rockford, IL) in a medium containing 250 mM sucrose, 10 mM HEPES, and 2 mM $KH_2PO_4$ (pH 7.4) (adjusted with Tris-base) at 25°C, as previously described (20, 46). Mitochondria (0.5 mg/ml) were energized by 10 mM succinate with 1 μM rotenone and pulsed with 50 μM $Ca^{2+}$ every 1.5 min. Maximal CRC was defined as the amount of $Ca^{2+}$ (per milligram of protein) required to induce spontaneous release of pre-accumulated $Ca^{2+}$.

### Mitochondrial respiration

Mitochondrial respiration was measured by recording oxygen consumption at 25°C in a chamber equipped with a Clark-type oxygen electrode (Instech Laboratories, Plymouth Meeting, PA), as previously described (14). Briefly, mitochondria were incubated in the medium containing 80 mM KCl, 50 mM MOPS, 1 mM EGTA, and 5 mM $KH_2PO_4$ (pH 7.4 adjusted by KOH) with complex I substrate (mixture of 5 mM glutamate and 5 mM malate). Maximal oxidative phosphorylation (state 3) was attained by addition of 500 μM ADP, and uncoupled respiration (state 3u) was measured in the presence of 50 μM 2,4-dinitrophenol (DNP).

### Western blot

Mitochondria or tissue samples were lysed in a buffer containing 50 mM Tris-HCl (pH 7.4), 5 mM EDTA, 150 mM NaCl, 1% Triton X-100, 1 mM $Na_3VO_4$, and 10 mM NaF, supplemented with a protease inhibitor cocktail (Roche, Indianapolis, IN). After 1 h on ice, lysates were centrifuged at 15,000 *g* for 10 min to remove insoluble material. Protein samples were then prepared by boiling lysates in reducing SDS-sample buffer. Thirty

micrograms of total proteins from each lysate were loaded onto 4–20% gradient SDS polyacrylamide gels, subjected to electrophoresis, and then transferred to polyvinylidene difluoride membranes, and blocked with 5% nonfat dry milk in TBS-T buffer [10 mM Tris, 150 mM NaCl, and 0.2% Tween 20 (pH 8.0)] overnight at 4°C. The blots were subsequently probed with appropriate primary antibodies, followed by horseradish peroxidase-labeled secondary antibody. Immunoreactive bands were visualized using a SuperSignal West Dura substrate (ThermoScientific, Rockford, IL). Relative band intensity was quantified using a Gel Doc EZ imager equipped with Quantify One software (Bio-Rad).

### Mitochondrial sphingolipids and diacylglycerol measurements

Mitochondrial sphingolipid and diacylglycerol species were determined by MS/MS (47). To extract lipids, 1 mg of mitochondrial protein was added to 2 ml of the ethyl acetate/isopropanol/water (60:30:10%, v/v/v) solvent system. The lipid extracts were fortified with internal standards, dried under a stream of nitrogen gas, and reconstituted in 100 μl of methanol for ESI-MS/MS analysis, which was performed on a Thermo-Fisher TSQ Quantum triple quadrupole mass spectrometer, operating in a multiple reaction-monitoring positive-ionization mode.

The samples were injected onto the HP1100/TSQ Quantum liquid chromatography/MS system and gradient-eluted from the BDS Hypersil C8, 150 × 3.2 mm, 3 μm particle size column, with a 1.0 mM methanolic ammonium formate, 2 mM aqueous ammonium formate mobile-phase system. The peaks for the target analytes and internal standards were collected and processed with the Xcalibur software system. Calibration curves were constructed by plotting peak area ratios of synthetic standards, representing each target analyte, to the corresponding internal standard. The target analyte peak area ratios from the samples were similarly normalized to their respective internal standard and compared with the calibration curves using a linear regression model.

### CerS activity assay

CerS activity was monitored by the formation of ceramide from sphingosine in the presence of palmitoyl-CoA or arachidoyl-CoA. To enhance the sensitivity of the assay, we employed synthetic 17C-sphingosine instead of natural 18C-sphingosine as a substrate, and 17C-ceramides formed in reaction were measured using MS/MS (9, 14). Mitochondria (0.5 mg/ml) were incubated with or without fumonisin B1 (FB1) for 5 min in a medium containing 250 mM sucrose, 5 μM rotenone, and 10 mM HEPES (pH 7.4 adjusted by KOH) at 37°C. Ceramide formation was initiated by addition of substrates and allowed to progress for 15 min. The reaction was terminated and ceramides were extracted by addition of 0.5 ml of the sample to 2 ml of the ethyl acetate/isopropanol/water (60:30:10%, v/v/v) solvent system, and the extracts were processed as described in the Mitochondrial sphingolipids and diacylglycerol measurements section above.

### Sphingolipid-metabolizing enzyme array

A custom PCR array of the sphingolipid-metabolizing gene network was developed by SA Biosciences (Valencia, CA) in collaboration with Dr. Christopher J. Clarke (Stony Brook University) (10). Primers were designed against the cDNA regions of the genes. Actin and GAPDH were utilized as reference genes. mRNA was extracted from tissue samples using a RNA Easy kit (Qiagen, Germantown, MD). RNA (0.5–1 μg) was used to synthesize cDNA with the SuperScript II kit for the first strand synthesis. Real-time RT-PCR was performed on a Bio-Rad MiniOpticon detection system. To run the assay, a MasterMix of 637.5 μl of SYBR-green, 51 μl of cDNA, and 586.5 μl of distilled water was prepared for each cDNA template. Twenty-five microliters were loaded per well. The RT-PCR protocol consisted of 10 min at 95°C for polymerase activation followed by 40 cycles of 15 s melt at 95°C and 60 s at 60°C for annealing and extension. After the cycles were run, a melt curve was performed to confirm a single product for each primer pair. The data were analyzed utilizing the PCR array data analysis portal at the SA Biosciences website.

### Statistical analysis

Data were collected, and the mean value of the treatment groups and the standard error were calculated. Data were analyzed for statistically significant differences by Student's *t*-test using Sigma Plot software (version 12.5). Statistical significance was ascribed to the data when $P < 0.05$.

## RESULTS

### Diabetes alters cardiac functions

Echocardiographic measurements of diabetic mice (**Table 1**) show that cardiac systolic function was altered in the diabetic mice compared with controls. LV EF and SV were significantly decreased in the diabetic hearts compared with controls. Additionally, the LA dimension was used as an index of chronic changes in LV diastolic function. LA dimensions were significantly increased in diabetic mice compared with controls, indicating sustained increased LV diastolic pressure. Overall, based on EF and SV measurement, it is possible to conclude that LV systolic function is decreased in diabetic mice compared with controls. In addition, based on LA dimension measurements, it is possible to say that LV diastolic function is altered in the diabetic mice. These pathological changes are in line with previously reported cardiac dysfunction in this particular model of STZ-induced diabetes (33, 36).

### Induction of diabetes increases expression of de novo ceramide-producing pathway enzymes without substantial changes in mitochondrial ceramide profile

The levels and turnover of sphingolipids are regulated by sphingolipid metabolizing enzymes (**Fig. 2**) that play essential roles in the shaping of sphingolipid signaling effects and cell responses (7, 8, 48, 49). The effect of diabetes on the sphingolipid enzyme gene expression network was examined using a PCR array in heart samples from diabetic animals (**Fig. 3**). Analysis of sphingolipid-metabolizing enzyme gene expression indicated that, of the 43 genes investigated, only 5 genes exhibited an upregulation of ⩾2-fold: *N*-acylethanolamine acid amidase (Naaa), acid ceramidase (Asah 1), (dihydro)ceramide synthase 2 (CerS2 or Lass 2), desaturase 1 (Degs 1), and galactosidase (Gla). Western blot analysis confirmed upregulation of CerS2 protein level in heart homogenates from diabetic mice (**Fig. 4A, B**). Interestingly, induction of diabetes also upregulated CerS2 content in the SSM (Fig. 4C, D). On mRNA level, expression of SPT subunits, the enzyme which catalyzes the initial step in the de novo pathway of ceramide formation, had not been changed. However, protein analysis showed increased abundance of SPTLC1

TABLE 1. Echocardiographic assessment of mice after 5 weeks of diabetes

| Group | BW (g) | HW/BW (mg/g) | HR (bpm) | LVW/BW (mg/g) | LV EF, (%) | LV SV (μl) | LA Dimension (mm) |
|---|---|---|---|---|---|---|---|
| Control | 25.6 ± 0.7 | 4.2 ± 0.13 | 492 ± 14 | 3.1 ± 0.2 | 59.5 ± 1.1 | 33.3 ± 1.3 | 1.8 ± 0.1 |
| Diabetic | 21.1 ± 0.6[a] | 4.0 ± 0.10 | 471 ± 25 | 2.8 ± 0.2 | 54.8 ± 1.0[a] | 28.4 ± 1.3* | 2.3 ± 0.1[a] |

Values are expressed as mean ± SEM (n = 6). BW, body weight in grams; HW, heart weight; HR, heart rate in beats per minute.

[a]$P < 0.05$ versus control using unpaired Student's *t*-test with two tail distribution.

in diabetic heart lysates (Fig. 4A, B). SPTLC1 anchors SPTLC1/SPTLC2 and SPTLC1/SPTLC3 heterodimers to the membrane, and is indispensable for the activity of these complexes. Therefore, an increased expression level of SPTLC1 can result in activation of SPT upon induction of diabetes. Induction of diabetes did not change expression of NCDase, either in heart lysates or in mitochondria. Abundance of glucosylceramide synthase (UGCG) was slightly decreased, which is in line with PCR array data.

CerS catalyzes ceramide formation from (dihydro) sphingosine and acyl-CoA, which can be blocked by FB1, a potent CerS inhibitor. Ceramide is also produced via FB1-insensitive reversed ceramidase reaction (9, 50, 51) from sphingosine and a fatty acid, which is formed in mitochondria as a result of hydrolysis of acyl-CoAs by thioesterase Acot2 (MTE-1) (9, 34, 52). The effect of diabetes on the activity of ceramide-generating enzymes was evaluated in cardiac mitochondria (**Fig. 5**). Control SSM readily formed ceramide from sphingosine and palmitoyl-CoA (Fig. 5A) or arachidoyl-CoA (Fig. 5C) in a FB1-sensitive manner, which attests for the activity of CerS in this mitochondrial fraction. Formation of ceramide by FB1-insensitive activity constituted about 20% of CerS activity with palmitoyl-CoA, and 17% with arachidoyl-CoA. Diabetic SSM displayed a 52 and 71% increase in CerS activity (FB1-sensitive component) for palmitoyl-CoA and arachidoyl-CoA, respectively. With arachidoyl-CoA, the FB1-insensitive component was increased 2.8 times. In contrast, this activity did not change while using palmitoyl-CoA as a substrate. In control IFM, FB1-sensitive CerS activity was 2-fold less with palmitoyl-CoA, and 4.8-fold less with arachidoyl-CoA, as compared with SSM (Fig. 3B, D). Diabetes did not significantly affect these activities in IFM. However, the results obtained with IFM should be interpreted cautiously. An isolation of IFM includes proteolytic treatment of the cardiac tissue with trypsin to separate mitochondria from myofibrils. Such treatment could separate the mitochondria from associated membranes [mitochondria-associated membranes (MAMs)] by disrupting tethering between the ER and mitochondria (53, 54) and inactivating CerS activity in the ER (55) and in the outer mitochondrial membrane. Therefore, the data suggest that only the CerS localized in the trypsin-inaccessible compartment of IFM did not respond to the induction of diabetes.

The increased gene/protein expression of desaturase 1, CerS2, and SPTLC1, along with increased mitochondrial CerS activity, are indicative of an activation of ceramide biosynthesis in diabetic heart. At the same time, activation of ceramide production did not translate to a substantial increase in ceramide content in mitochondria (**Fig. 6**).

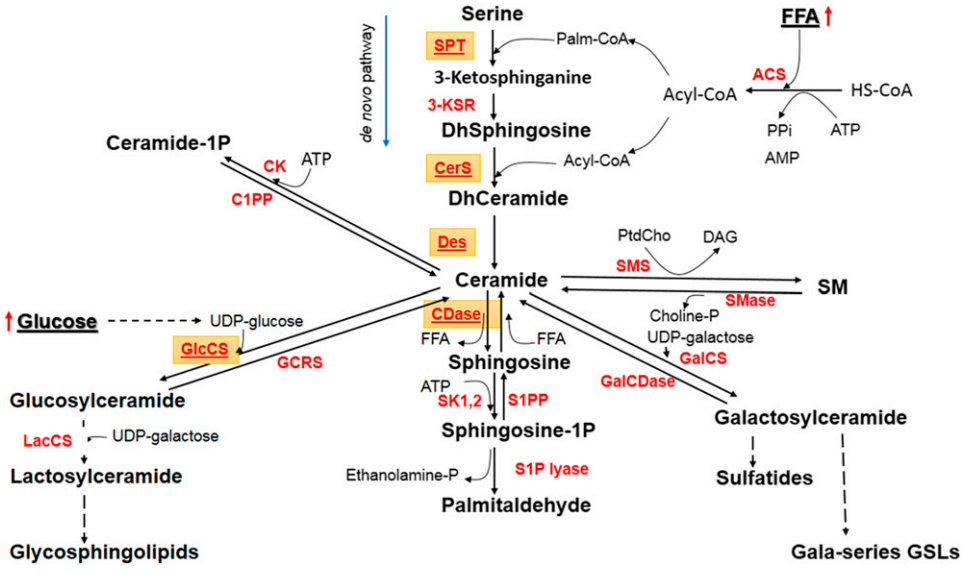


**Fig. 2.** Ceramide-centered model of sphingolipid metabolism. ACS, acyl-CoA synthase; CDase, ceramidase; CK, ceramide kinase; C1PP, ceramide-1P phosphatase; Des, desaturase; GlcCS, glucosylceramide synthase; GCRS, glucocerebrosidase; GalCS, galactosylceramide synthase; GalCDase, galactosylceramidase; 3-KSR, 3-ketosphinganine reductase; LacCS, lactosylceramide synthase; SK1,2, sphingosine kinases 1 and 2; S1PP, S1P phosphatase; SMS, SM synthase. Highlighted are differentially expressed enzymes and enzymes under consideration.

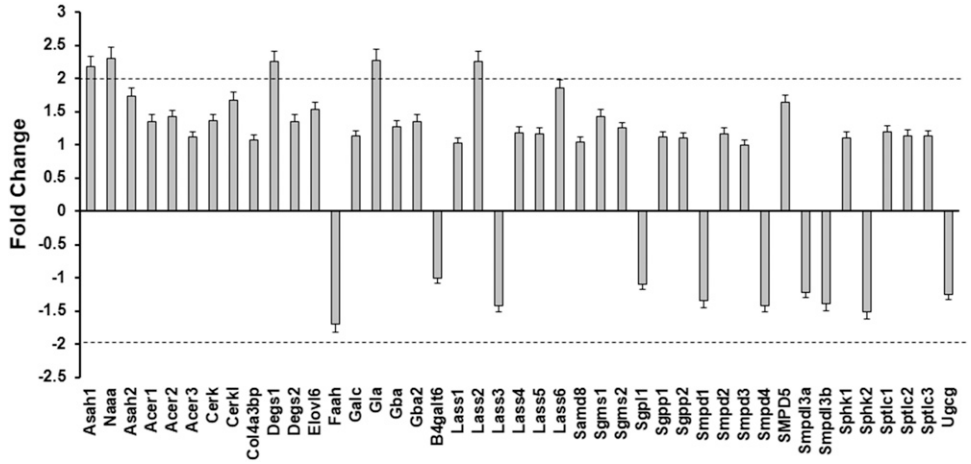


**Fig. 3.** Sphingolipid-metabolizing enzyme's gene expression after induction of diabetes. Heart samples were prepared from control and diabetic mice. RNA was extracted and converted to cDNA for analysis by real-time PCR using a PCR array as described in the Materials and Methods. The data are presented as a fold change comparing diabetes to control and are the means of three independent experiments. The dashed line represents a 2-fold change.

Although, among major ceramides, $C_{20:0}$-ceramide was significantly increased (34%) in SSM, there was no change in other major ceramides, including $C_{16:0}$-, $C_{18:0}$-, $C_{18:1}$-, $C_{20:1}$, $C_{22:0}$-, $C_{22:1}$-, $C_{24:0}$-, and $C_{24:1}$-ceramide species (Fig. 6A) and minor ceramides ($C_{14:0}$-, $C_{20:4}$-, $C_{26:0}$-, and $C_{26:1}$-ceramides; not shown), resulting in only a 17% increase in total ceramide in SSM (**Fig. 7A**). There were no changes in ceramide species in IFM (Fig. 6B) and in total ceramide upon induction of diabetes (Fig. 7A). The lack of a substantial increase in mitochondrial ceramide, despite an upregulation of ceramide biosynthesis, suggests concomitant upregulation of ceramide-metabolizing activities.

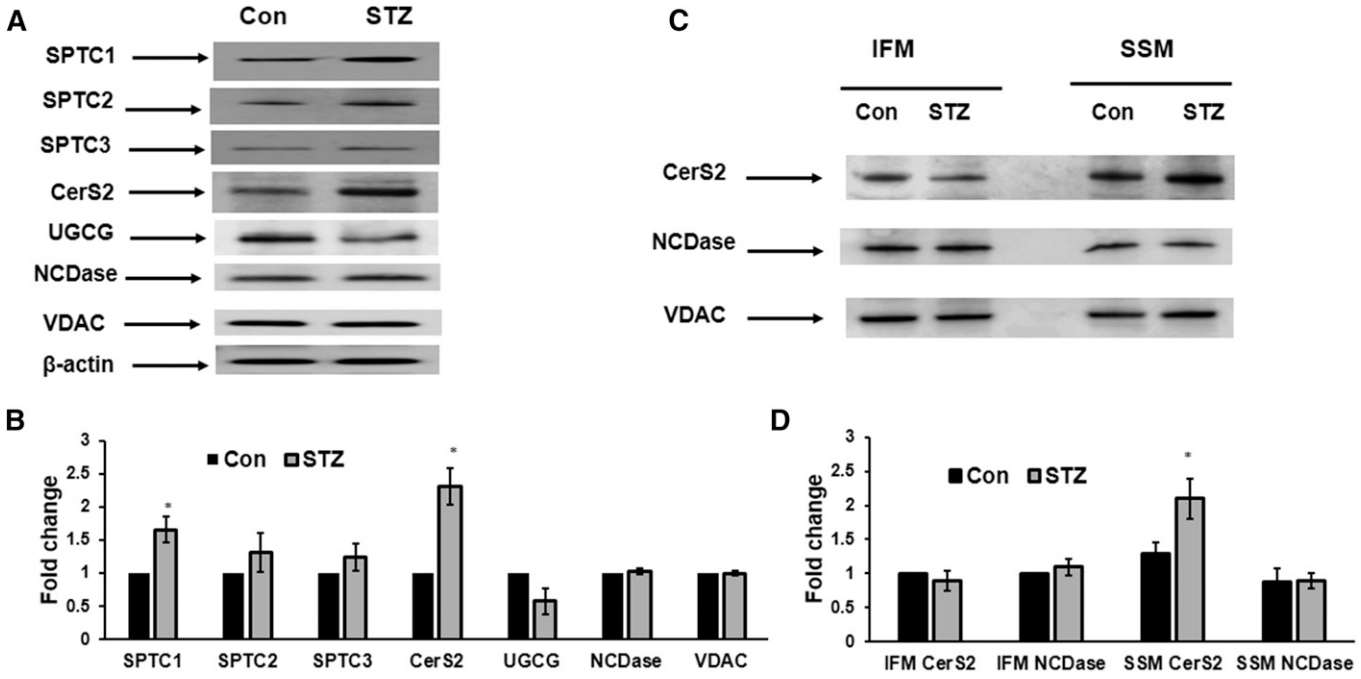


**Fig. 4.** Effect of diabetes on the abundance of ceramide metabolizing enzymes in heart lysates (A, B) and isolated mitochondria (C, D). Western blots were performed by loading equal amounts of 30 μg of homogenate (A), or mitochondrial (SSM or IFM) protein per lane, except VDAC, which was assessed using protein loading of 15 μg per lane. A: Representative Western blot of heart lysates. B: Quantification of protein expression in heart lysates. Levels of respective proteins were normalized against β-actin and their expression in STZ animals relative to control was determined. Data are mean ± SE of three homogenate preparations; eight to ten mice were used for each preparation of homogenate. $*P < 0.05$. C: Representative Western blot of heart mitochondria. D: Quantification of protein expression in heart mitochondria. Levels of respective proteins were normalized against VDAC and their expression relative to IFM control was determined. Data are mean ± SE of three preparations; eight to ten mice were used for each preparation of mitochondria. $*P < 0.05$.

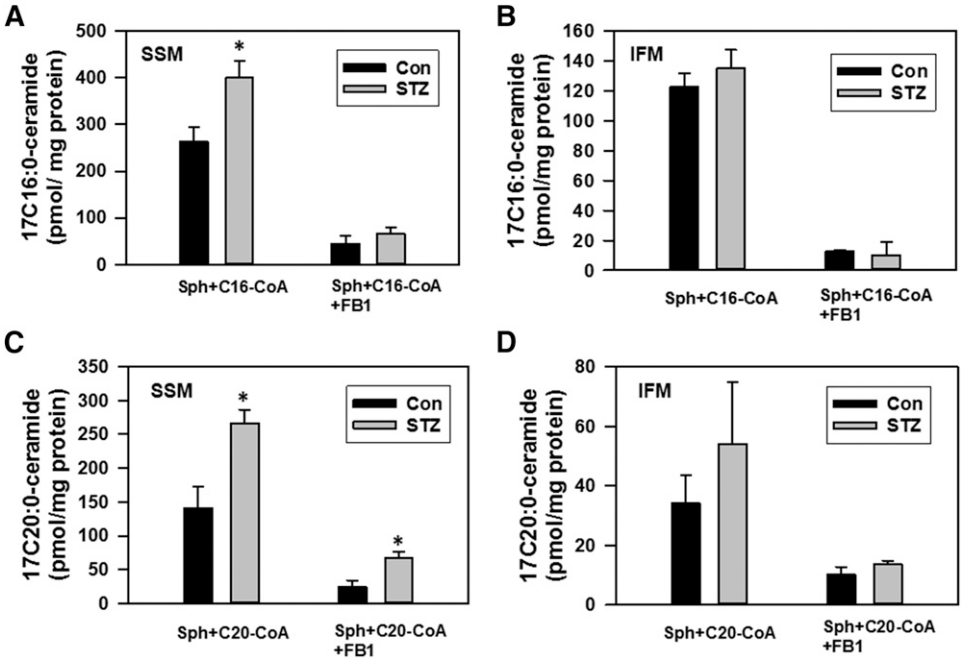


**Fig. 5.** Effect of diabetes on ceramide biosynthesis in SSM (A, C) and IFM (B, D) fractions. Mitochondria (0.5 mg/ml) were incubated as indicated with 50 μM palmitoyl-CoA (C16:0-CoA) or 50 μM arachidoyl-CoA (C20:0-CoA) in the presence of 15 μM 17C-sphingosine under conditions described in the Materials and Methods for 15 min before the reaction was terminated by addition of ethyl acetate/isopropyl alcohol extraction mixture. When present, FB1 was added to the medium at 50 μM. The results represent the mean ± SE (n = 3). *$P < 0.05$.

### Increased ceramide hydrolysis by NCDase counterbalances de novo ceramide formation upon induction of diabetes

One of the major pathways of ceramide utilization is its hydrolysis by ceramidases, which are comprised of a heterogenic family of enzymes which include acid ceramidase (ASAH1), NCDase (ASAH2), and three alkaline ceramidases (ACER1, ACER2, and ACER3) (56). Acid ceramidase is localized to the lysosomes. There is a diverse localization of alkaline ceramidases: ACER1 is localized to the ER and is mainly expressed in the skin, ACER2 is localized to the Golgi, and ACER3 is localized to both the Golgi and ER. Although NCDase was thought to preferentially localize to the plasma membrane, accumulating evidence demonstrates the presence of NCDase activity, or the enzyme itself (depending on the tissue/cell studied), in endosomal/lysosomal compartments (57) and mitochondria (9–11, 58). In our previous studies, we have shown that mitochondria-resident NCDase modulates the ceramide profile of liver mitochondria (9). Therefore, in the present studies aimed at assessment of a relationship between mitochondrial sphingolipid metabolism and mitochondrial functions upon induction of diabetes, we focused our attention on NCDase. To determine the NCDase contribution to shaping the ceramide profile of mitochondria from diabetic heart, we utilized NCDase KO mice. Knocking down NCDase resulted in increased ceramide species (Fig. 6C, D) and total ceramide (Fig. 7A) in both SSM and IFM from a baseline heart, attesting that mitochondrial NCDase is involved in clearance of mitochondrial ceramide. Upon induction of diabetes in the NCDase-deficient mice, ceramide increases were greater compared with the WT mice for both SSM (52.6 pmol/mg for WT vs. 111.3 pmol/mg protein for NCDase KO) and IFM (23.5 pmol/mg for WT vs. 119.5 pmol/mg protein for NCDase KO). These increases cover all major ceramide species (Fig. 6C, D). The data suggest that diabetes increases ceramide flux in cardiac mitochondria, which is controlled, at least in part, by mitochondrial NCDase.

### Diabetes increases mitochondrial lactosylceramide

To evaluate other potential pathways of ceramide utilization, the sphingolipid profile was determined in mitochondria from diabetic heart (Fig. 7). SM, the end-metabolic product of ceramide utilization, was considerably elevated both in SSM and IFM (43%, or by 1,157.4 pmol/mg protein, and 37.8%, or by 861.7 pmol/mg protein, respectively; Fig. 7D). Knocking down NCDase did not change total SM in either WT or NCDase KO SSM from diabetic heart, whereas SM was slightly increased in IFM compared with WT. There were only minor changes in diacylglycerol levels in mitochondria and homogenates from WT and KO diabetic hearts (**Fig. 8**). Hexosylceramides were not increased upon induction of diabetes (Fig. 7C), although it should be noted that knocking down NCDase substantially (92%) increased total hexosylceramide in IFM, specifically $C_{22:0}$-, $C_{24:0}$-, and $C_{24:1}$-hexosylceramide species. In contrast, lactosylceramide was highly elevated both in SSM and IFM in diabetic heart (Fig. 7B; **Fig. 9A, B**).

Total lactosylceramide was increased by 38% (Fig. 7B), with substantial increases in $C_{18:0}$-, $C_{20:0}$-, and $C_{22:0}$-lactosylceramide species (Fig. 9A) in SSM from diabetic WT mice

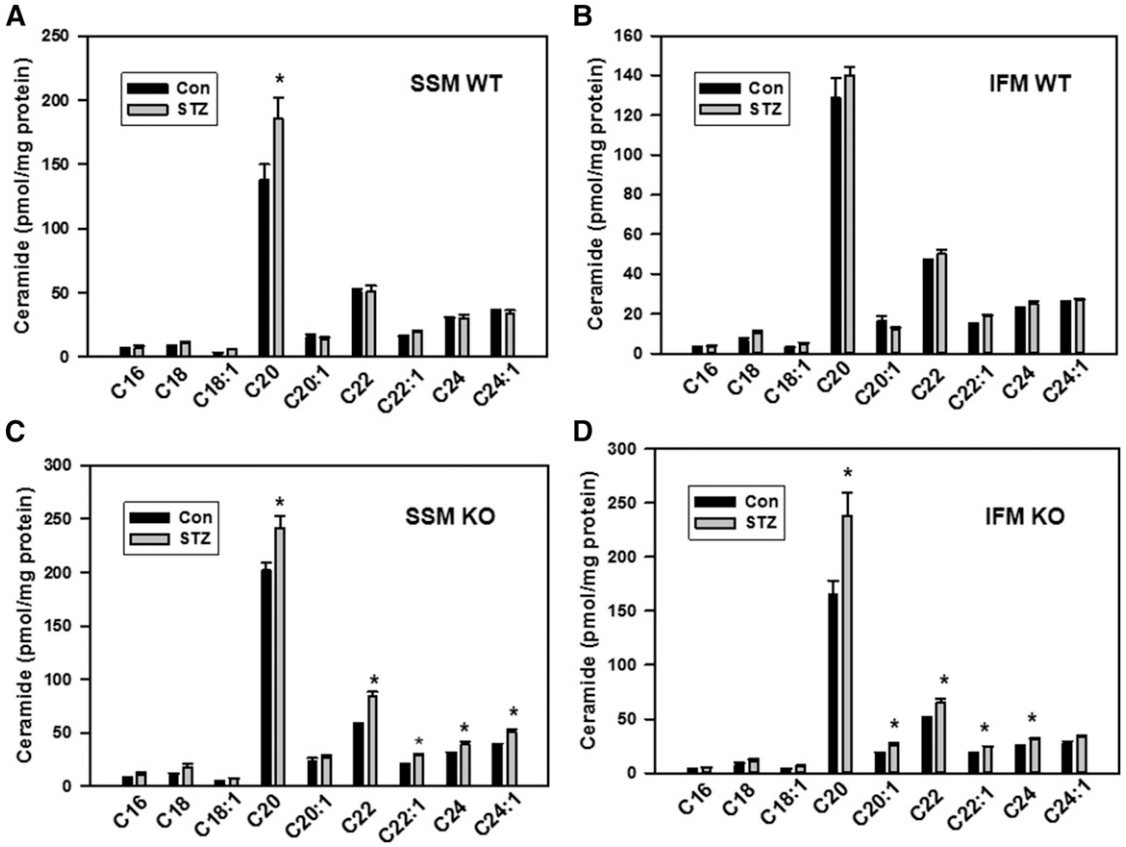


**Fig. 6.** Changes in major mitochondrial ceramide species in diabetic hearts of WT (A, B) and NCDase KO (C, D) mice. The results represent the mean ± SE (n = 3). *$P < 0.05$.

compared with controls. In IFM from diabetic WT mice, total lactosylceramide was increased by 65% (Fig. 7B), with significant increases in $C_{18:0}$-, $C_{20:0}$-, $C_{22:0}$-, and $C_{24:0}$-lactosylceramide species (Fig. 9B). Knocking down NCDase resulted in a more than 2-fold increase in total lactosylceramide level in IFM from diabetic heart compared with WT (Fig. 7B), suggesting a crosstalk between glucosylceramide synthase- and NCDase-mediated ceramide utilization pathways.

### Knocking down NCDase exacerbates mitochondrial dysfunction in diabetic heart

It was reported that mitochondria from STZ-induced diabetic mouse hearts display a decreased state 3 respiration (34–36) and an increased propensity for mPTP opening in response to oxidative stress (39). **Figure 10** shows the decreased glutamate/malate supported state 3 respiration both in SSM (by 26%) and IFM (by 25%), while state 4 has not been affected. This decrease in state 3 respiration seems to reflect the inhibition of maximal electron transport by respiratory chain because of the concomitant decrease in DNP-uncoupled respiration (state 3u). Inhibition of state 3 respiration, which is supported by complex I substrates in IFM, after the induction of diabetes with STZ in mice, was somewhat less than reported for diabetic rat [37–39% for rat SSM (34, 35); 39–55% for rat IFM (34)]. Moreover, there was no change in SSM and a 37% decrease for IFM from the hearts of mice with FAV genetic background (36). Because, in the present studies, mice with C57BL/6 genetic background were used, the differences might be species/strain related. Importantly, knocking down NCDase decreases state 3 and state 3u respiration similar to diabetes, and the induction of diabetes in NCDase KO mice further exacerbates this effect. Thus, the maximal suppression of state 3 respiration was observed in NCDase KO diabetic animals, as compared with WT controls: in SSM by 33% and in IFM by 43%.

We further assessed the effect of diabetes on the CRC of SSM and IFM. Mitochondria respiring on succinate were challenged with 50 μM $Ca^{2+}$ pulses every 90 s until the onset of spontaneous $Ca^{2+}$ release. The amount of $Ca^{2+}$ accumulated before this threshold is termed CRC and reflects a propensity of mPTP to adopt an open state. A comparison of traces 1 and 2 (**Fig. 11A**), obtained with WT baseline mitochondria, shows that SSM have a decreased CRC compared with IFM, which is in line with previously published data (59). This decrease in CRC reflects an increased sensitivity of mPTP in SSM to $Ca^{2+}$. Indeed, the addition of the mPTP inhibitor, cyclosporin A (CSA), to SSM drastically improved the CRC (trace 3). Induction of diabetes decreased CRC of WT IFM by 35%, while having minor effect on SSM (Fig. 11B). Knocking down NCDase by itself decreases CRC in control IFM by 31%, with a maximal decrease observed in diabetic NCDase KO mice of 49% compared with WT controls.

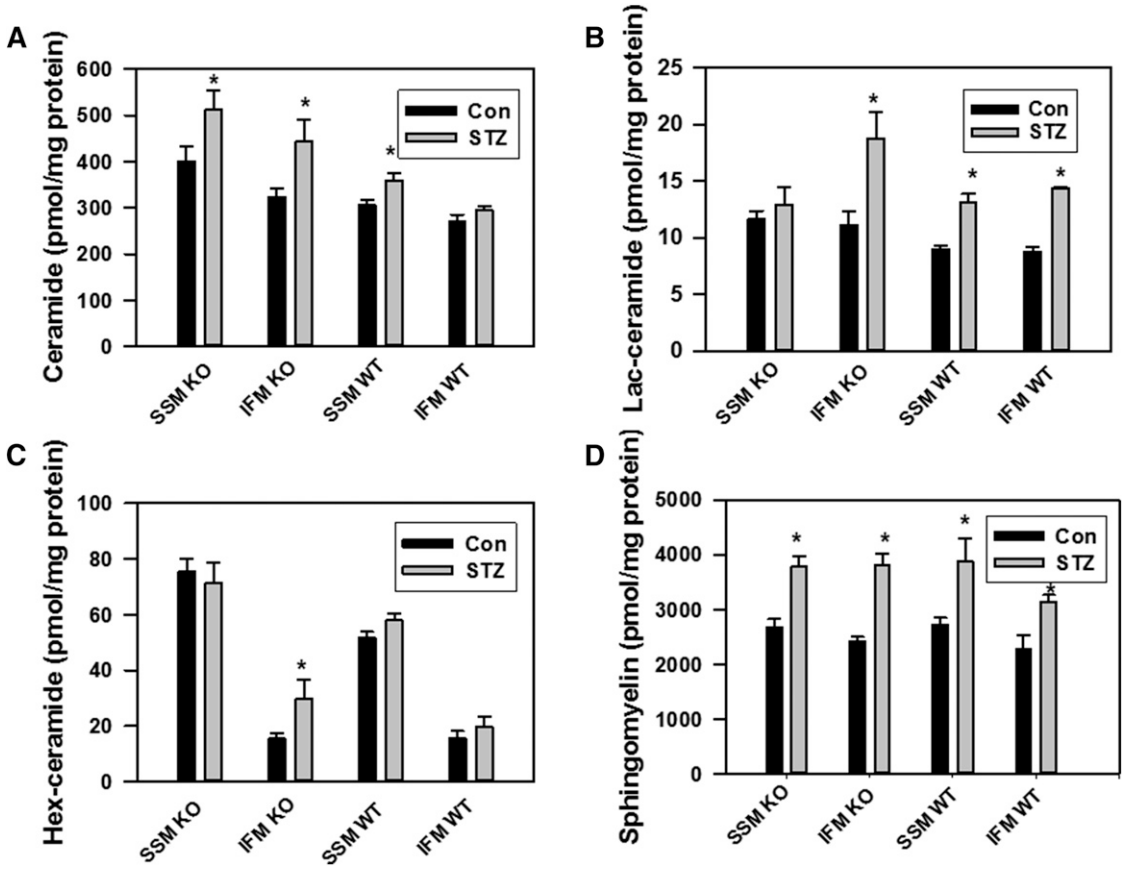


**Fig. 7.** Sphingolipid profile of mitochondria in diabetic hearts of WT and NCDase KO mice. A: Changes in total ceramide. B: Changes in total lactosylceramide. C: Changes in total hexosylceramide. D: Changes in total SM. The results represent the mean ± SE (n = 3). *$P <$ 0.05.

**Lactosylceramide suppresses mitochondrial respiration and decreases CRC**

To determine whether the diabetes-induced mitochondrial dysfunction was mediated by accumulated lactosylceramide, we examined the impact of lactosylceramide on the mitochondrial respiratory chain activity and CRC in baseline cardiac mitochondria. An addition of 100 μM of $C_{16:0}$-lactosylceramide to IFM respiring on complex I substrate glutamate/malate in the presence of ADP (state 3) resulted in rapid suppression of respiration (**Fig. 12A**, trace 3 as compared with control trace 1). Subsequent addition of uncoupler DNP did not accelerate respiration, indicating a respiratory chain defect. Ceramides can release cytochrome c by promoting formation of large channels in the outer mitochondrial membrane that results in the suppression of respiration caused by release of cytochrome c (18). However, an addition of 10 μM exogenous cytochrome c to mitochondria failed to reverse the inhibition of respiratory chain activity exerted by lactosylceramide, which seems to exclude this mechanism (Fig. 12A, trace 3). $C_{16:0}$-glucosylceramide at 100 μM had only minor effect on respiration (Fig. 12A, trace 2), indicating a high degree of specificity of the lactosylceramide binding site on the mitochondrial respiratory chain.

In contrast to mitochondria respiring on glutamate/malate, where $C_{16:0}$-lactosylceramide potently suppressed state 3 respiration with $IC_{50}$ = 20.7 μM, state 3 respiration supported by complex II (succinate) or complex IV [*N,N,N′,N′*-tetramethyl-*p*-phenelenediamine (TMPD)+ ascorbate] substrates was affected to a lesser extent (Fig. 12B). The data suggest complex I as the primary target for the lactosylceramide.

Besides the effect on the respiratory chain, $C_{16:0}$-lactosylceramide also decreased mitochondrial ability to retain the

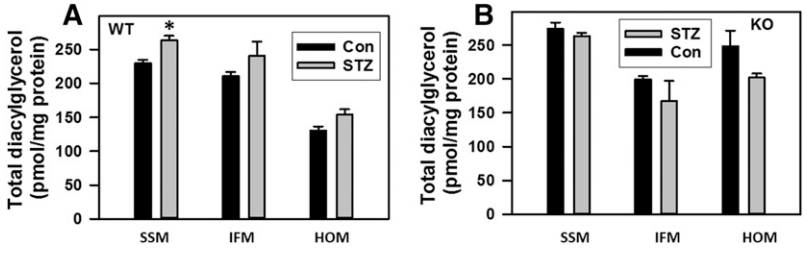


**Fig. 8.** Changes in total values of mitochondrial diacylglycerol in diabetic hearts of WT (A) and NCDase KO (B) mice. The results represent the mean ± SE (n = 3). *$P <$ 0.05.

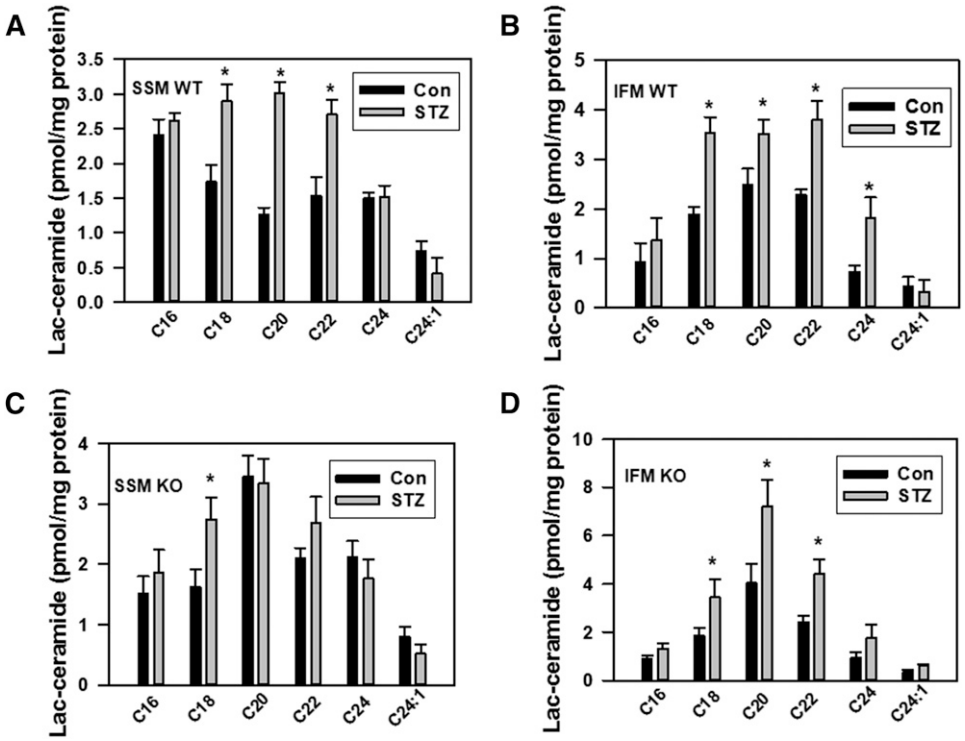


**Fig. 9.** Changes in mitochondrial lactosylceramide species in diabetic hearts of WT (A, B) and NCDase KO (C, D) mice. The results represent the mean ± SE (n = 3). *$P < 0.05$.

accumulated $Ca^{2+}$. **Figure 13A** demonstrates a decreased CRC of IFM (trace 2) in the presence of 50 μM of $C_{16:0}$-lactosylceramide as compared with the control (trace 1). This effect is due to an increased sensitivity of mPTP to $Ca^{2+}$, not to the inability of mitochondria to accumulate it because of the dysfunctional respiratory chain. Indeed, mPTP inhibitor CSA restores CRC to the original value (trace 3).

An additional confirmation of mPTP opening by $C_{16:0}$-lactosylceramide comes from the evaluation of mitochondrial light scattering responses (Fig. 13B), which were measured simultaneously with monitoring $Ca^{2+}$ (Fig. 13A). An injection of mitochondria to the medium resulted in a limited decrease in light scattering (swelling), which presumably originates from limited entry of $K^+$ into the matrix space, because it was not observed in sucrose-containing medium (not shown) (Fig. 13B, trace 1). Readings remained stable during subsequent $Ca^{2+}$ pulses until mitochondria started to undergo a high amplitude swelling indicative of mPTP opening. In the presence of $C_{16:0}$-lactosylceramide, the high amplitude swelling was initiated at lower levels of accumulated $Ca^{2+}$ (Fig. 13B, trace 2) that was prevented by CSA (trace 3). The data suggest that lactosylceramide could enhance the mPTP sensitivity to $Ca^{2+}$.

Of note, $C_{16:0}$-lactosylceramide was added to the medium simultaneously with mitochondria, and this addition resulted in a more pronounced immediate decrease in light scattering, as compared with the control. In contrast to the delayed high amplitude swelling, which corresponded to spontaneous $Ca^{2+}$ release, the initial light scattering response was not sensitive to CSA (Fig. 13B, trace 3) and seemed to represent a modulation of structural topology of the mitochondrial membrane by $C_{16:0}$-lactosylceramide (60, 61). Overall, the mitochondrial dysfunction in diabetic heart tissue is accompanied by the accumulation of lactosylceramide, which could mimic the effect of diabetes in baseline cardiac mitochondria.

## DISCUSSION

Cardiomyopathy in type 1 diabetes was repeatedly linked to mitochondrial dysfunction and the accumulation of

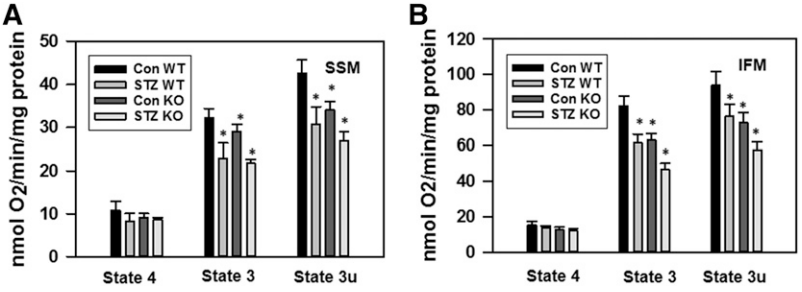


**Fig. 10.** Diabetes suppresses state 3 and state 3u respiration both in SSM (A) and IFM (B). Mitochondria (0.5 mg/ml) were incubated at conditions described in the Materials and Methods. State 3 was initiated by addition of 500 μM ADP; state 3u was initiated by addition of 50 μM DNP; state 4 represents respiration in ADP-free conditions. The results represent the mean ± SE (n = 3). *$P < 0.05$ versus WT control.

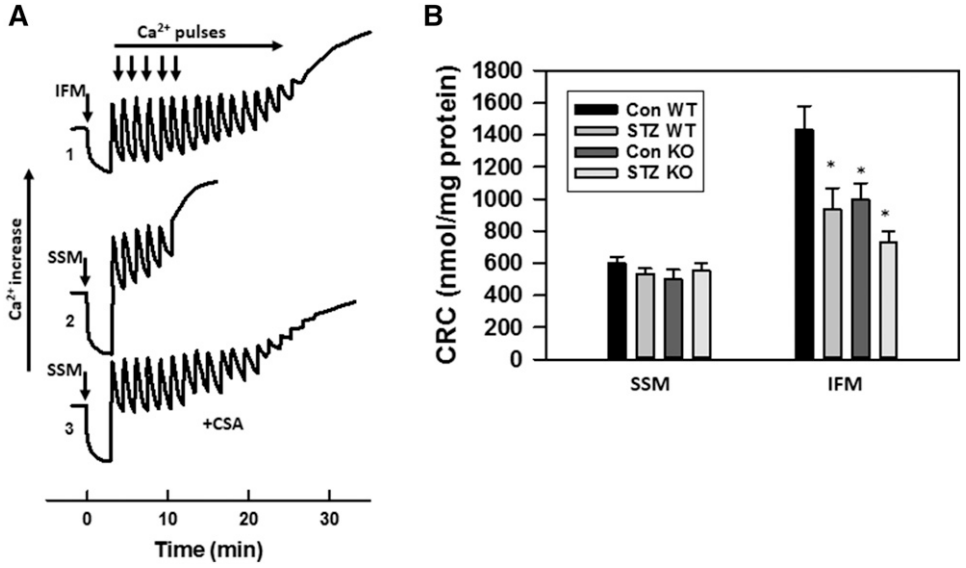


**Fig. 11.** Diabetes decreases CRC of IFM, attesting for increased sensitivity of mPTP to $Ca^{2+}$. A: Representative $Ca^{2+}$ traces of the assessment of CRC in baseline WT IFM (trace 1) and SSM (trace 2) determined as described in the Materials and Methods. Mitochondria (0.5 mg/ml) were challenged with 50 μM $Ca^{2+}$ pulses every 90 sec. CRC of SSM determined in the presence of 2 μM CSA (trace 3). B: Effect of diabetes on CRC of SSM and IFM. The results represent the mean ± SE (n = 3). $*P < 0.05$.

toxic lipids, among which ceramide, a pro-apoptotic sphingolipid, plays an essential role. Despite mounting evidence related to the deleterious effect of ceramide on mitochondrial function in vitro, there is a gap in our knowledge as to whether any substantial changes in the mitochondrial profile of ceramide or its derivatives occur in diabetic heart tissue and what biochemical mechanisms underlie the mitochondrial dysfunction. However, a decrease in SM was reported in the total mitochondrial fraction from the hearts of STZ-induced diabetic rats (62).

In this study, we provide evidence that ceramide is not a major factor in mitochondrial dysfunction in the hearts of diabetic mice, but rather its metabolite, lactosylceramide, contributes to injury. Indeed, ceramide content did not change considerably in both SSM and IFM upon induction of diabetes, but ceramide flux was substantially increased, i.e., the activation of ceramide-producing pathways was counterbalanced by the simultaneous upregulation of ceramide-metabolizing pathways. Some of the increase in ceramide level in mitochondria from WT mice

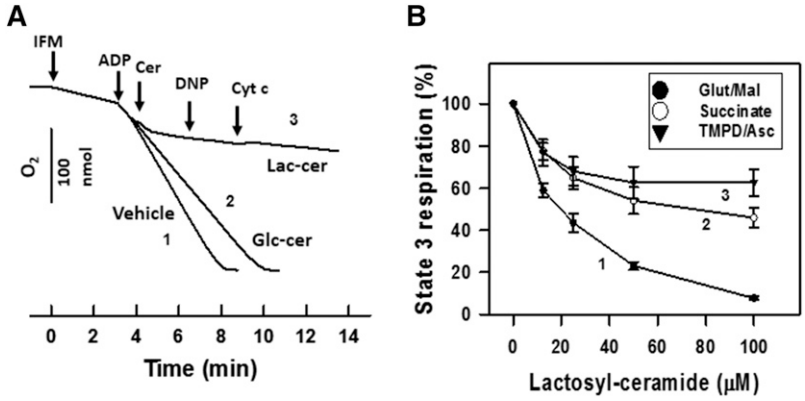


**Fig. 12.** Exogenous lactosylceramide, but not glucosylceramide, suppresses mitochondrial respiration in baseline mitochondria. A: Mitochondria (0.5 mg/ml) were incubated as described in the Materials and Methods in the medium supplemented with glutamate/malate (5 mM each). State 3 respiration was initiated by addition of 2 mM ADP. Trace 1, vehicle control; trace 2, 100 μM $C_{16:0}$-glucosylceramide was introduced as indicated; trace 3, 100 μM $C_{16:0}$-lactosylceramide was added. In trace 3, 50 μM DNP and 10 μM cytochrome c were introduced as indicated. B: Dose-response curves of lactosylceramide inhibiting state 3 respiration rate in the presence of complex I substrate [5 mM glutamate/malate (trace 1)], complex II substrate [10 mM succinate plus 2 μM rotenone (trace 2)], or complex IV substrate [1 mM ascorbate/250 μM TMPD plus antimycin at 2μg/mg protein (trace 3)]. Mitochondria were first preincubated for 6 min in the presence of the indicated concentrations of $C_{16:0}$-lactosyceramide, then respiration state 3 was initiated by simultaneous addition of the indicated substrate and 2 mM ADP.

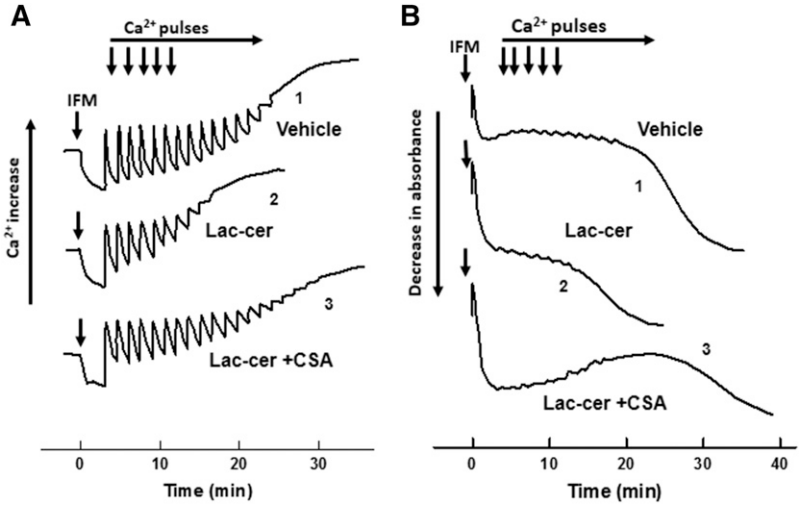


**Fig. 13.** Exogenous lactosylceramide decreases CRC and potentiates high-amplitude swelling of baseline IFM in a CSA-sensitive manner. WT mitochondria (0.5 mg/ml) were incubated in succinate-supplemented respiratory medium devoid of EGTA. Mitochondria were challenged with 50 μM $Ca^{2+}$ pulses every 90 s. Changes in $Ca^{2+}$ concentration in the medium (A) and mitochondrial swelling (B) were determined simultaneously. Trace 1, vehicle control; trace 2, 50 μM of $C_{16:0}$-lactosylceramide was added simultaneously with mitochondria; trace 3, 50 μM $C_{16:0}$-lactosylceramide in the presence of 2 μM CSA.

could potentially originate from suppression of NCDase upon induction of diabetes. However, there was no increase of NCDase on protein level (Fig. 4), either in heart lysates (Fig. 4A, B) or in mitochondria (Fig. 4C, D). Although, murine NCDase can be glycosylated with N- and O-glycans (56), which might affect ceramidase activity, we think that NCDase specifically clears ceramide originating from the de novo pathway at the same rate in both control and diabetic animals. Ablation of NCDase interrupts this clearance, leading to increased ceramide level.

It was reported that suppression of the particular ceramide metabolizing pathway affects other pathways in the ceramide-metabolizing network, causing a change in the levels of other metabolites or a significant shift in particular metabolite species (22, 63). Kono et al. (43) have shown that ablation of NCDase does not markedly affect either total ceramide level or particular ceramide species in heart at basal conditions, indicating lack of activation of compensatory pathways. However, in our experiments, we observed an increase in total ceramide content in mitochondria from NCDase KO mice at basal conditions (29% in SSM and 19% in IFM) without significant changes in ceramide species profile. This increase was not accompanied by a change in total SM. In contrast to the SM pathway, this rise in ceramide translates to its increased tunneling to glycosphingolipids, as indicated by the increased content of glycosylceramide (46% in SSM; although no changes in IFM were detected) and lactosylceramide (~28% both for SSM and IFM).

Upon induction of diabetes, increased expression of desaturase 1, CerS2, and SPTLC1 (Figs. 3, 4), as well as increased CerS activity in mitochondria (Fig. 5), indicated enhanced ceramide biosynthesis as a plausible source of mitochondrial ceramide. Besides, increased availability of the substrates for the formation of ceramide and lactosylceramide should also contribute to the increased sphingolipid metabolism. Elevated levels of FFA contribute to increased ceramide formation (64–66). In STZ-induced diabetes, the lack of insulin releases suppression of lipolysis in adipocytes (67, 68), resulting in elevated levels of FFA in plasma (69–72), accompanied by expression of FFA transporters, CD36 and FATP1, in sarcolemma (2, 73). This facilitates the transport of FFAs into cytosol where they are rapidly converted to acyl-CoAs, thus raising their levels (69). Acyl-CoAs are immediate substrates for SPT and CerS, which are the critical enzymes in ceramide formation by the de novo pathway (Fig. 2). At the same time, increased glucose promotes formation of UDP-glucose and UDP-galactose, the substrates for glucosylceramide and lactosylceramide synthases, which tunnel newly formed ceramides to glucosylceramides and further to lactosylceramides. Lactosylceramide, within our model, is one of the causative factors in mitochondrial dysfunction. Active AMPK suppresses glucosylceramide synthase and reduces the level of glucosylceramide in the cell (74). So, decreased AMPK activity observed in STZ-induced diabetic heart (75) is an additional factor that accelerates formation of glycosphingolipids. Perturbation in intracellular $Ca^{2+}$ homeostasis resulting from decreased expression/activity of sarco/ER calcium ATPase (SERCA) and compromised mitochondrial $Ca^{2+}$ handling in STZ-induced diabetic hearts (76) can potentially modulate ceramide metabolism. However, variations in activity of SERCA and mitochondrial $Ca^{2+}$ controlling mPTP opening/closure do not affect the levels of diacylglycerol or ceramide (77, 78). This suggests that deregulation of $Ca^{2+}$ homeostasis and mPTP activity is likely downstream of ceramide metabolism, or they are independent factors.

Our finding that an increased ceramide flux promotes mitochondrial dysfunction is further supported by studies using NCDase-deficient mice. Knocking out NCDase increased ceramide levels in mitochondria upon induction of diabetes, as compared with the controls (Figs. 6, 7), attesting, first, that ceramide flux is increased, and, second, that NCDase acts as a safety mechanism preventing ceramide build up above physiological level.

This is in contrast to liver mitochondria, where reversed NCDase activity in concert with thioesterase is a primary source of mitochondrial ceramide formation from palmitoyl-CoA and sphingosine (9). As shown in Fig. 5, the reverse activity of NCDase in heart mitochondria is considerably less than the activity of CerS.

A similar phenomenon was reported by Gorski and colleagues for the myocardium of type 2 diabetic patients where, despite of an increase in apoptotic markers, ceramide level was unchanged compared with controls (79, 80). At the same time, activation of the enzymes involved in both ceramide formation (neutral SMase, SPT) and ceramide utilization (ceramidases, sphingosine kinase 1) occurred in concert, suggesting an elevated rate of ceramide turnover. These data were interpreted as an indication that ceramide is not a major contributor to cardiomyocyte apoptosis; however, the involvement of ceramide metabolites has not been ruled out. Indeed, Kester and colleagues have reported an ~30% increase in glucosylceramide mass in the retinas of STZ-induced diabetic rats at the expense of an ~30% decrease of ceramide mass (81). Based on pharmacological studies with R28 retinal neurons, they came to the conclusion that it is glucosylceramide formed from ceramide by glucosylceramide synthase or downstream glycosphingolipids derived from glucosylceramide that are causative factors for cell death in diabetic retinopathy. These data are in line with our results demonstrating a substantial increase in lactosylceramide, the immediate downstream product of glucosylceramide, both in the SSM and IFM of diabetic animals.

Western blotting shows some downregulation of glucosylceramide synthase (UGCG) protein expression (Fig. 4A), which is in agreement with mRNA measurements. This is in apparent discrepancy with observed elevated levels of lactosylceramide. However, this contradiction can be resolved in the framework of results reported by Shayman and colleagues (82) for STZ-induced diabetic kidney. They showed that the apparent $K_m$ of glucosylceramide synthase for UDP-glucose is 250 μM in both normal and diabetic animals. At the same time, the estimated concentration of UDP-glucose is 149 μM in normal tissue. Therefore, glucosylceramide synthase is far from saturated with the substrate, and availability of UDP-glucose is a rate limiting step. Upon induction of diabetes, UDP-glucose rises up to 237 μM, thus driving increased formation of glucosylceramide. We think that in our case, some decrease in glucosylceramide synthase content is overcompensated by increased availability of the substrates (UDP-glucose and ceramide) to drive the reaction toward formation of glucosylceramide, and subsequently to lactosylceramide. In the same article, it was reported that an increase in glucosylceramide content is accompanied by a simultaneous increase in ganglioside GM3, which suggests that in diabetes, the overall reaction is shifted to anabolism of glycosphingolipids.

Another ceramide-utilizing pathway involved in maintaining the mitochondrial ceramides at a steady level upon induction of diabetes is SM formation. There was a substantial increase in SM content in STZ-treated mice, both in SSM and IFM (Fig. 7D), that is in contrast to the previously reported SM decrease in total mitochondria preparation from diabetic rat heart (62). However, knocking down NCDase resulted in a minor further increase of SM content in IFM. SM content in SSM was not affected at all. This suggests that the SM pool, in contrast to lactosylceramide, is not in direct equilibrium with the pool of ceramide accessible to NCDase, and that the increase in SM in mitochondrial subpopulations of diabetic hearts reflects a suppression of SM hydrolysis rather than activation of SM synthesis. In line with this notion, there is no evidence of the SM synthase presence in mitochondria, but a novel mitochondria-associated neutral SMase has been cloned and characterized (12, 13, 83).

In models of lipotoxic cardiomyopathy (64) and in the Akita mouse model of type 1 diabetes (1), cardiac levels of diacylglycerol increase in parallel with ceramide. In our model, there was no substantial increase in diacylglycerol content in SSM, IFM, or homogenates upon induction of diabetes (Fig. 8). So, it seems that changes in mitochondrial diacylglycerol content cannot explain observed suppression of respiratory chain and sensibilization of mPTP. This is in line with the lack of direct effect of diacylglycerol on the mitochondrial respiratory chain, at least at the level of complex IV (22). At the same time, it is plausible that a local rise in diacylglycerol in extra mitochondrial compartments activates PKC, which in turn indirectly affects mitochondrial function. This question awaits further investigation.

The origin and metabolism of ceramide in mitochondria is less obscure. Although the initial steps and the majority of de novo ceramide formation clearly take place in the ER (7, 8), the enzymes involved in the final steps of ceramide formation (CerS and dihydroceramide desaturase) were also found in mitochondria (14, 84, 85). Moreover, Ardail and colleagues provided evidence that MAM, the specialized ER compartment involved in the transfer of lipids and $Ca^{2+}$ between the ER and mitochondria (86–88), contains glucosylceramide and lactosylceramide synthases which tunnel glycosphingolipids to mitochondria (89). On the catabolic side of ceramide metabolism, mitochondrial association of NCDase (9–11) and sphingosine kinase 2 (10, 15) were also demonstrated. It is conceivable that mitochondria and MAM form a specialized compartment of sphingolipid metabolism providing sphingolipid species to modulate the mitochondrial function in a context-specific manner.

Although ceramide, among other sphingolipids, is considered to be a major factor regulating respiratory chain activity and mPTP (16, 17, 19–21) in type 1 diabetes, the diabetes-induced suppression of respiratory chain activity (Fig. 10) and the decrease in CRC (Fig. 11) are accompanied by increased levels of lactosylceramide. This suggests that glycosphingolipids could modulate mitochondrial functions in diabetes. Indeed, in vitro experiments with ganglioside GD3 displayed its role in the induction of mPTP followed by cytochrome c release, a suppression of respiratory chain activity, and enhanced ROS production (26–28). The evidence of lactosylceramide involvement in mitochondrial dysfunction is limited. Lactosylceramide was reported to enhance ROS production in isolated mitochondria respiring on succinate (28), which is consistent with inhibition of the respiratory chain at the level of complex III or complex IV (90). In our studies, the lactosylceramide suppressed the state 3 respiration supported by

substrates of complex I (glutamate/malate), complex II (succinate), and complex IV (TMPD/ascorbate) (Fig. 12). Similar suppression of state 3 respiration in the presence of either succinate or TMPD/ascorbate suggests that lactosylceramide blocked the electron transport in the respiratory chain at the level of complex IV. However, more potent inhibition of state 3 respiration supported by glutamate/malate points to complex I as a preferred target of lactosylceramide. The inhibition of respiration is not due to mPTP opening with subsequent cytochrome c release, as was shown for GD3 ganglioside (26), because the mitochondrial incubation medium was depleted of $Ca^{2+}$, an essential mPTP activator, by the presence of EGTA. A specific permeabilization of the outer mitochondrial membrane for cytochrome c by lactosylceramide, as was demonstrated for ceramide (18), seems unlikely. Indeed, an addition of exogenous cytochrome c did not restore the respiration rate to the original level (Fig. 12A). The data suggest that lactosylceramide can directly inhibit respiratory chain complexes I and IV.

The ability of lactosylceramide to enhance ROS production presumably originated from the inhibition of the respiratory chain in isolated mitochondria (28), which is of special interest in light of elevated levels of markers for oxidative stress both in SSM and IFM from the hearts of STZ-induced diabetic mice (e.g., nitrosine-containing proteins as a markers for protein oxidative modification, and malondialdehyde and 4-hydroxyalkenal as a markers for lipid peroxidation) (33, 36). Moreover, these studies have shown an increased rate of production of superoxide by IFM from diabetic mice, which is in line with recently published data by Rosca and colleagues demonstrating increased ROS production by SSM from STZ-induced diabetic rat heart (91). Although the increased number of mitochondria observed in the hearts from chronic models of type 1 diabetes (OVE26 and Akita mice) (92, 93) can potentially contribute to overall cellular ROS production, in STZ-induced diabetic heart, no change in mitochondrial content was detected (91). Therefore, it seems more plausible that disturbance of ROS production in STZ-induced diabetes does not originate from alteration of the mitochondrial content in particular cells, but rather from defects in the mitochondrion itself. This increase in mitochondria-associated oxidative stress was suggested to be one of the underlying causes of diabetic cardiomyopathy.

Another mitochondrial dysfunction associated with diabetes is the ability of mitochondria to retain accumulated $Ca^{2+}$. The CRC of IFM determined in an incubation medium devoid of EGTA showed a decreased capacity of mitochondria to accumulate and retain $Ca^{2+}$ in the presence of lactosylceramide, which can be restored in the presence of the mPTP inhibitor, CSA (Fig. 13B). This suggests that lactosylceramide could increase the sensitivity of mPTP to $Ca^{2+}$. However, simultaneous measurements of mitochondrial light scattering in the time-course of CRC determination showed more complex changes (Fig. 10). The addition of lactosylceramide to mitochondria resulted in an immediate CSA-insensitive decrease in light scattering, followed by a delayed CSA-sensitive decrease in light scattering. The CSA-sensitive light scattering phase coincides well with the initiation of $Ca^{2+}$ release from mitochondria and undoubtedly reflects the mPTP opening. The nature of the acute light scattering response to lactosylceramide remains obscure. Future studies should clarify the nature of the structural topology changes in mitochondrial membranes caused by lactosylceramide and whether its biophysical behavior is involved in modulation of mitochondrial functional activities.

Lactosylceramide is a precursor of many gangliosides. Ardail et al. (89) have shown the presence of sialyltransferase activities in MAM. Addition of sialic acid to lactosylceramide is the first step in the formation of gangliosides. We cannot completely exclude the presence of residual MAM in our preparation, which is below the detection level of Western blot. However, mitochondrial incubation medium does not contain substrates for the formation of gangliosides, such as CMP-*N*-acetylneuraminic (sialic) acid or UDP-*N*-acetylgalactosamine (94). Therefore, it is safe to conclude that in isolated mitochondria, effects should be ascribed to lactosylceramide itself, but not to the subsequent formation of gangliosides. At the cellular level, Shayman and coworkers (82) detected an increased level of GM3 in the kidneys of STZ-induced diabetic rats, indicating favorable conditions for the formation of gangliosides. Increased ganglioside formation was also observed under hyperglycemic conditions in R28 cells (81). This potentially indicates that the MAM/mitochondria fraction might also increase ganglioside production in response to diabetic challenge. However, in isolated mitochondria, GM3 along with GM1, GD1, GD1a, and GT1 were absolutely ineffective in the induction of mPTP (26, 27, 95). Among all the gangliosides tested, only GD3 potentiates mPTP opening. Reports on the effect of gangliosides on the mitochondrial respiratory chain are missing, except for GD3, which suppresses respiration by releasing cytochrome c caused via permeability transition (26). Therefore, we cannot exclude that higher-level glycosphingolipids, along with lactosylceramide, potentially contribute to mitochondrial dysfunction. Further work will be required for assessment of the effect of particular ganglioside species on mitochondrial function, and the discrimination of the effects of lactosylceramide and gangliosides on mitochondria upon induction of diabetes.

There is another limitation of this study. To confirm whether lactosylceramide is the major species involved in mitochondrial dysfunction in diabetic heart, modulation of lactosylceramide synthesis would be desirable. To decrease lactosylceramide synthesis in diabetic mice, we utilized the glucosylceramide synthase inhibitor, D-*threo*-PDMP, according to the procedure of Hisaki et al. (96), who reported an increase in ceramide levels in the brain, indicative glucosylceramide synthase suppression. In a similar protocol, Shayman and colleagues (82) observed reversal of diabetic nephropathy by D-*threo*-PDMP in STZ-induced diabetic rats. However, we did not detect significant changes in hexosylceramide or lactosylceramide levels in heart mitochondrial fractions from diabetic

animals upon D-*threo*-PDMP treatment. The lack of the changes of lactosylceramide in mitochondria can indicate a very low turnover rate of this molecule in the mitochondria/MAM fraction or in the heart of STZ-diabetic animals compared with brain and kidney. Another possibility is that these protocols did not provide a sufficient concentration of D-*threo*-PDMP in the heart to suppress glucosylceramide synthase. Developing new strategies to suppress lactosylceramide accumulation in mitochondria and defining the potential role of higher-level glycosphingolipids would provide more detail for understanding the contribution of glycosphingolipids to mitochondrial dysfunction in diabetic heart tissue. However, these questions have need of separate dedicated studies.

Overall, the present work demonstrates that mitochondrial dysfunction in STZ-induced diabetic heart correlates with accumulation of lactosylceramide, and that lactosylceramide exogenously added to baseline mitochondria reproduces diabetic phenotype. The results of our studies suggest that the elevated lactosylceramide may be one of the initial causative factors of mitochondrial dysfunction in type 1 diabetes. Diabetes-induced accumulation of lactosylceramide results in the inhibition of respiratory chain activity, leading to increased ROS production (28), which, in turn, impairs the mitochondrial protein import machinery, assembly of respiratory chain complexes (36), and mPTP opening. This further exacerbates cellular oxidative stress and promotes cardiac damage.

Our results highlight the novel role of glycosphingolipids in the pathobiology of diabetes and identify the enzymes involved in the modulation of glycosphingolipid metabolism that could serve as promising pharmacological targets for correction of mitochondrial abnormalities in type 1 diabetes.

The authors thank Mr. Alexander S. Novgorodov for help with preparation of the manuscript.

## REFERENCES


1. Basu, R., G. Y. Oudit, X. Wang, L. Zhang, J. R. Ussher, G. D. Lopaschuk, and Z. Kassiri. 2009. Type 1 diabetic cardiomyopathy in the Akita (Ins2WT/C96Y) mouse model is characterized by lipotoxicity and diastolic dysfunction with preserved systolic function. *Am. J. Physiol. Heart Circ. Physiol.* **297:** H2096–H2108.
2. Kuramoto, K., F. Sakai, N. Yoshinori, T. Y. Nakamura, S. Wakabayashi, T. Kojidani, T. Haraguchi, F. Hirose, and T. Osumi. 2014. Deficiency of a lipid droplet protein, perilipin 5, suppresses myocardial lipid accumulation, thereby preventing type 1 diabetes-induced heart malfunction. *Mol. Cell. Biol.* **34:** 2721–2731.
3. Russo, S. B., J. S. Ross, and L. A. Cowart. 2013. Sphingolipids in obesity, type 2 diabetes, and metabolic disease. *Handb. Exp. Pharmacol.* **216:** 373–401.
4. Wende, A. R., and E. D. Abel. 2010. Lipotoxicity in the heart. *Biochim. Biophys. Acta.* **1801:** 311–319.
5. Park, T. S., and I. J. Goldberg. 2012. Sphingolipids, lipotoxic cardiomyopathy, and cardiac failure. *Heart Fail. Clin.* **8:** 633–641.
6. Boudina, S., and E. D. Abel. 2010. Diabetic cardiomyopathy, causes and effects. *Rev. Endocr. Metab. Disord.* **11:** 31–39.
7. Hannun, Y. A., and L. M. Obeid. 2008. Principles of bioactive lipid signalling: lessons from sphingolipids. *Nat. Rev. Mol. Cell Biol.* **9:** 139–150.
8. Lahiri, S., and A. H. Futerman. 2007. The metabolism and function of sphingolipids and glycosphingolipids. *Cell. Mol. Life Sci.* **64:** 2270–2284.
9. Novgorodov, S. A., B. X. Wu, T. I. Gudz, J. Bielawski, T. V. Ovchinnikova, Y. A. Hannun, and L. M. Obeid. 2011. Novel pathway of ceramide production in mitochondria: thioesterase and neutral ceramidase produce ceramide from sphingosine and acyl-CoA. *J. Biol. Chem.* **286:** 25352–25362.
10. Novgorodov, S. A., C. L. Riley, J. Yu, K. T. Borg, Y. A. Hannun, R. L. Proia, M. S. Kindy, and T. I. Gudz. 2014. Essential roles of neutral ceramidase and sphingosine in mitochondrial dysfunction due to traumatic brain injury. *J. Biol. Chem.* **289:** 13142–13154.
11. El Bawab, S., P. Roddy, T. Qian, A. Bielawska, J. J. Lemasters, and Y. A. Hannun. 2000. Molecular cloning and characterization of a human mitochondrial ceramidase. *J. Biol. Chem.* **275:** 21508–21513.
12. Wu, B. X., V. Rajagopalan, P. L. Roddy, C. J. Clarke, and Y. A. Hannun. 2010. Identification and characterization of murine mitochondria-associated neutral sphingomyelinase (MA-nSMase), the mammalian sphingomyelin phosphodiesterase 5. *J. Biol. Chem.* **285:** 17993–18002.
13. Rajagopalan, V., D. Canals, C. Luberto, J. Snider, C. Voelkel-Johnson, L. M. Obeid, and Y. A. Hannun. 2015. Critical determinants of mitochondria-associated neutral sphingomyelinase (MA-nSMase) for mitochondrial localization. *Biochim. Biophys. Acta.* **1850:** 628–639.
14. Yu, J., S. A. Novgorodov, D. Chudakova, H. Zhu, A. Bielawska, J. Bielawski, L. M. Obeid, M. S. Kindy, and T. I. Gudz. 2007. JNK3 signaling pathway activates ceramide synthase leading to mitochondrial dysfunction. *J. Biol. Chem.* **282:** 25940–25949.
15. Strub, G. M., M. Paillard, J. Liang, L. Gomez, J. C. Allegood, N. C. Hait, M. Maceyka, M. M. Price, Q. Chen, D. C. Simpson, et al. 2011. Sphingosine-1-phosphate produced by sphingosine kinase 2 in mitochondria interacts with prohibitin 2 to regulate complex IV assembly and respiration. *FASEB J.* **25:** 600–612.
16. Novgorodov, S. A., and T. I. Gudz. 2009. Ceramide and mitochondria in ischemia/reperfusion. *J. Cardiovasc. Pharmacol.* **53:** 198–208.
17. Kogot-Levin, A., and A. Saada. 2014. Ceramide and the mitochondrial respiratory chain. *Biochimie.* **100:** 88–94.
18. Colombini, M. 2013. Membrane channels formed by ceramide. *Handb. Exp. Pharmacol.* **215:** 109–126.
19. Roy, S. S., M. Madesh, E. Davies, B. Antonsson, N. Danial, and G. Hajnoczky. 2009. Bad targets the permeability transition pore independent of Bax or Bak to switch between Ca2+-dependent cell survival and death. *Mol. Cell.* **33:** 377–388.
20. Novgorodov, S. A., T. I. Gudz, and L. M. Obeid. 2008. Long-chain ceramide is a potent inhibitor of the mitochondrial permeability transition pore. *J. Biol. Chem.* **283:** 24707–24717.
21. Novgorodov, S. A., Z. M. Szulc, C. Luberto, J. A. Jones, J. Bielawski, A. Bielawska, Y. A. Hannun, and L. M. Obeid. 2005. Positively charged ceramide is a potent inducer of mitochondrial permeabilization. *J. Biol. Chem.* **280:** 16096–16105.
22. Zigdon, H., A. Kogot-Levin, J. W. Park, R. Goldschmidt, S. Kelly, A. H. Merrill, Jr., A. Scherz, Y. Pewzner-Jung, A. Saada, and A. H. Futerman. 2013. Ablation of ceramide synthase 2 causes chronic oxidative stress due to disruption of the mitochondrial respiratory chain. *J. Biol. Chem.* **288:** 4947–4956.
23. Hassoun, S. M., S. Lancel, P. Petillot, B. Decoster, R. Favory, P. Marchetti, and R. Neviere. 2006. Sphingosine impairs mitochondrial function by opening permeability transition pore. *Mitochondrion.* **6:** 149–154.
24. Scorrano, L., D. Penzo, V. Petronilli, F. Pagano, and P. Bernardi. 2001. Arachidonic acid causes cell death through the mitochondrial permeability transition. Implications for tumor necrosis factor-alpha apoptotic signaling. *J. Biol. Chem.* **276:** 12035–12040.
25. Broekemeier, K. M., and D. R. Pfeiffer. 1995. Inhibition of the mitochondrial permeability transition by cyclosporin A during long time frame experiments: relationship between pore opening and the activity of mitochondrial phospholipases. *Biochemistry.* **34:** 16440–16449.
26. Scorrano, L., V. Petronilli, F. Di Lisa, and P. Bernardi. 1999. Commitment to apoptosis by GD3 ganglioside depends on opening of the mitochondrial permeability transition pore. *J. Biol. Chem.* **274:** 22581–22585.
27. Kristal, B. S., and A. M. Brown. 1999. Apoptogenic ganglioside GD3 directly induces the mitochondrial permeability transition. *J. Biol. Chem.* **274:** 23169–23175.
28. García-Ruiz, C., A. Colell, R. París, and J. C. Fernández-Checa. 2000. Direct interaction of GD3 ganglioside with mitochondria generates reactive oxygen species followed by mitochondrial permeability transition, cytochrome c release, and caspase activation. *FASEB J.* **14:** 847–858.

29. Anderson, E. J., E. Rodriguez, C. A. Anderson, K. Thayne, W. R. Chitwood, and A. P. Kypson. 2011. Increased propensity for cell death in diabetic human heart is mediated by mitochondrial-dependent pathways. *Am. J. Physiol. Heart Circ. Physiol.* **300:** H118–H124.
30. Bugger, H., and E. D. Abel. 2010. Mitochondria in the diabetic heart. *Cardiovasc. Res.* **88:** 229–240.
31. Sivitz, W. I., and M. A. Yorek. 2010. Mitochondrial dysfunction in diabetes: from molecular mechanisms to functional significance and therapeutic opportunities. *Antioxid. Redox Signal.* **12:** 537–577.
32. Duncan, J. G. 2011. Mitochondrial dysfunction in diabetic cardiomyopathy. *Biochim. Biophys. Acta.* **1813:** 1351–1359.
33. Dabkowski, E. R., C. L. Williamson, V. C. Bukowski, R. S. Chapman, S. S. Leonard, C. J. Peer, P. S. Callery, and J. M. Hollander. 2009. Diabetic cardiomyopathy-associated dysfunction in spatially distinct mitochondrial subpopulations. *Am. J. Physiol. Heart Circ. Physiol.* **296:** H359–H369.
34. King, K. L., M. E. Young, J. Kerner, H. Huang, K. M. O'Shea, S. E. Alexson, C. L. Hoppel, and W. C. Stanley. 2007. Diabetes or peroxisome proliferator-activated receptor alpha agonist increases mitochondrial thioesterase I activity in heart. *J. Lipid Res.* **48:** 1511–1517.
35. Lashin, O. M., P. A. Szweda, L. I. Szweda, and A. M. Romani. 2006. Decreased complex II respiration and HNE-modified SDH subunit in diabetic heart. *Free Radic. Biol. Med.* **40:** 886–896.
36. Baseler, W. A., E. R. Dabkowski, R. Jagannathan, D. Thapa, C. E. Nichols, D. L. Shepherd, T. L. Croston, M. Powell, T. T. Razunguzwa, S. E. Lewis, et al. 2013. Reversal of mitochondrial proteomic loss in type 1 diabetic heart with overexpression of phospholipid hydroperoxide glutathione peroxidase. *Am. J. Physiol. Regul. Integr. Comp. Physiol.* **304:** R553–R565.
37. Oliveira, P. J., R. Seica, P. M. Coxito, A. P. Rolo, C. M. Palmeira, M. S. Santos, and A. J. Moreno. 2003. Enhanced permeability transition explains the reduced calcium uptake in cardiac mitochondria from streptozotocin-induced diabetic rats. *FEBS Lett.* **554:** 511–514.
38. Lumini-Oliveira, J., J. Magalhaes, C. V. Pereira, A. C. Moreira, P. J. Oliveira, and A. Ascensao. 2011. Endurance training reverts heart mitochondrial dysfunction, permeability transition and apoptotic signaling in long-term severe hyperglycemia. *Mitochondrion.* **11:** 54–63.
39. Williamson, C. L., E. R. Dabkowski, W. A. Baseler, T. L. Croston, S. E. Alway, and J. M. Hollander. 2010. Enhanced apoptotic propensity in diabetic cardiac mitochondria: influence of subcellular spatial location. *Am. J. Physiol. Heart Circ. Physiol.* **298:** H633–H642.
40. Sloan, R. C., F. Moukdar, C. R. Frasier, H. D. Patel, P. A. Bostian, R. M. Lust, and D. A. Brown. 2012. Mitochondrial permeability transition in the diabetic heart: contributions of thiol redox state and mitochondrial calcium to augmented reperfusion injury. *J. Mol. Cell. Cardiol.* **52:** 1009–1018.
41. Palmer, J. W., B. Tandler, and C. L. Hoppel. 1977. Biochemical properties of subsarcolemmal and interfibrillar mitochondria isolated from rat cardiac muscle. *J. Biol. Chem.* **252:** 8731–8739.
42. Hollander, J. M., D. Thapa, and D. L. Shepherd. 2014. Physiological and structural differences in spatially distinct subpopulations of cardiac mitochondria: influence of cardiac pathologies. *Am. J. Physiol. Heart Circ. Physiol.* **307:** H1–H14.
43. Kono, M., J. L. Dreier, J. M. Ellis, M. L. Allende, D. N. Kalkofen, K. M. Sanders, J. Bielawski, A. Bielawska, Y. A. Hannun, and R. L. Proia. 2006. Neutral ceramidase encoded by the Asah2 gene is essential for the intestinal degradation of sphingolipids. *J. Biol. Chem.* **281:** 7324–7331.
44. Zile, M. R., C. F. Baicu, R. E. Stroud, A. Van Laer, J. Arroyo, R. Mukherjee, J. A. Jones, and F. G. Spinale. 2012. Pressure overload-dependent membrane type 1-matrix metalloproteinase induction: relationship to LV remodeling and fibrosis. *Am. J. Physiol. Heart Circ. Physiol.* **302:** H1429–H1437.
45. Lang, R. M., Bierig, M., Devereux, R. B., Flachskampf, F. A., Foster, E., Pellikka, P. A., Picard, M. H., Roman, M. J., Seward, J., Shanewise, et al. 2005. Recommendations for chamber quantification: a report from the American Society of Echocardiography's Guidelines and Standards Committee and the Chamber Quantification Writing Group, developed in conjunction with the European Association of Echocardiography, a branch of the European Society of Cardiology. *J. Am. Soc. Echocardiogr.* **18:** 1440–1463.
46. Soriano, M. E., L. Nicolosi, and P. Bernardi. 2004. Desensitization of the permeability transition pore by cyclosporin a prevents activation of the mitochondrial apoptotic pathway and liver damage by tumor necrosis factor-alpha. *J. Biol. Chem.* **279:** 36803–36808.
47. Bielawski, J., Z. M. Szulc, Y. A. Hannun, and A. Bielawska. 2006. Simultaneous quantitative analysis of bioactive sphingolipids by high-performance liquid chromatography-tandem mass spectrometry. *Methods.* **39:** 82–91.
48. Patwardhan, G. A., L. J. Beverly, and L. J. Siskind. Sphingolipids and mitochondrial apoptosis. *J. Bioenerg. Biomembr.* Epub ahead of print. January 27, 2015; doi:10.1007/s10863-015-9602-3.
49. Garcia-Ruiz, C., A. Morales, and J. C. Fernandez-Checa. 2015. Glycosphingolipids and cell death: one aim, many ways. *Apoptosis.* **20:** 607–620.
50. Tani, M., N. Okino, S. Mitsutake, T. Tanigawa, H. Izu, and M. Ito. 2000. Purification and characterization of a neutral ceramidase from mouse liver. A single protein catalyzes the reversible reaction in which ceramide is both hydrolyzed and synthesized. *J. Biol. Chem.* **275:** 3462–3468.
51. El Bawab, S., H. Birbes, P. Roddy, Z. M. Szulc, A. Bielawska, and Y. A. Hannun. 2001. Biochemical characterization of the reverse activity of rat brain ceramidase. A CoA-independent and fumonisin B1-insensitive ceramide synthase. *J. Biol. Chem.* **276:** 16758–16766.
52. Gerber, L. K., B. J. Aronow, and M. A. Matlib. 2006. Activation of a novel long-chain free fatty acid generation and export system in mitochondria of diabetic rat hearts. *Am. J. Physiol. Cell Physiol.* **291:** C1198–C1207.
53. Csordás, G., C. Renken, P. Várnai, L. Walter, D. Weaver, K. F. Buttle, T. Balla, C. A. Mannella, and G. Hajnóczky. 2006. Structural and functional features and significance of the physical linkage between ER and mitochondria. *J. Cell Biol.* **174:** 915–921.
54. Chipuk, J. E., G. P. McStay, A. Bharti, T. Kuwana, C. J. Clarke, L. J. Siskind, L. M. Obeid, and D. R. Green. 2012. Sphingolipid metabolism cooperates with BAK and BAX to promote the mitochondrial pathway of apoptosis. *Cell.* **148:** 988–1000.
55. Hirschberg, K., J. Rodger, and A. H. Futerman. 1993. The long-chain sphingoid base of sphingolipids is acylated at the cytosolic surface of the endoplasmic reticulum in rat liver. *Biochem. J.* **290:** 751–757.
56. Mao, C., and L. M. Obeid. 2008. Ceramidases: regulators of cellular responses mediated by ceramide, sphingosine, and sphingosine-1-phosphate. *Biochim. Biophys. Acta.* **1781:** 424–434.
57. Mitsutake, S., M. Tani, N. Okino, K. Mori, S. Ichinose, A. Omori, H. Iida, T. Nakamura, and M. Ito. 2001. Purification, characterization, molecular cloning, and subcellular distribution of neutral ceramidase of rat kidney. *J. Biol. Chem.* **276:** 26249–26259.
58. Monette, J. S., L. A. Gomez, R. F. Moreau, K. C. Dunn, J. A. Butler, L. A. Finlay, A. J. Michels, K. P. Shay, E. J. Smith, and T. M. Hagen. 2011. (R)-alpha-Lipoic acid treatment restores ceramide balance in aging rat cardiac mitochondria. *Pharmacol. Res.* **63:** 23–29.
59. Holmuhamedov, E. L., A. Oberlin, K. Short, A. Terzic, and A. Jahangir. 2012. Cardiac subsarcolemmal and interfibrillar mitochondria display distinct responsiveness to protection by diazoxide. *PLoS One.* **7:** e44667.
60. Maggio, B., M. L. Fanani, C. M. Rosetti, and N. Wilke. 2006. Biophysics of sphingolipids II. Glycosphingolipids: an assortment of multiple structural information transducers at the membrane surface. *Biochim. Biophys. Acta.* **1758:** 1922–1944.
61. Westerlund, B., and J. P. Slotte. 2009. How the molecular features of glycosphingolipids affect domain formation in fluid membranes. *Biochim. Biophys. Acta.* **1788:** 194–201.
62. Ferreira, R., G. Guerra, A. I. Padrao, T. Melo, R. Vitorino, J. A. Duarte, F. Remiao, P. Domingues, F. Amado, and M. R. Domingues. 2013. Lipidomic characterization of streptozotocin-induced heart mitochondrial dysfunction. *Mitochondrion.* **13:** 762–771.
63. Mullen, T. D., S. Spassieva, R. W. Jenkins, K. Kitatani, J. Bielawski, Y. A. Hannun, and L. M. Obeid. 2011. Selective knockdown of ceramide synthases reveals complex interregulation of sphingolipid metabolism. *J. Lipid Res.* **52:** 68–77.
64. Park, T. S., Y. Hu, H. L. Noh, K. Drosatos, K. Okajima, J. Buchanan, J. Tuinei, S. Homma, X. C. Jiang, E. D. Abel, et al. 2008. Ceramide is a cardiotoxin in lipotoxic cardiomyopathy. *J. Lipid Res.* **49:** 2101–2112.
65. Turpin, S. M., G. I. Lancaster, I. Darby, M. A. Febbraio, and M. J. Watt. 2006. Apoptosis in skeletal muscle myotubes is induced by ceramides and is positively related to insulin resistance. *Am. J. Physiol. Endocrinol. Metab.* **291:** E1341–E1350.
66. Dyntar, D., M. Eppenberger-Eberhardt, K. Maedler, M. Pruschy, H. M. Eppenberger, G. A. Spinas, and M. Y. Donath. 2001. Glucose and palmitic acid induce degeneration of myofibrils and modulate apoptosis in rat adult cardiomyocytes. *Diabetes.* **50:** 2105–2113.

67. Jelenik, T., G. Sequaris, K. Kaul, D. M. Ouwens, E. Phielix, J. Kotzka, B. Knebel, J. Weiss, A. L. Reinbeck, L. Janke, et al. 2014. Tissue-specific differences in the development of insulin resistance in a mouse model for type 1 diabetes. *Diabetes.* **63:** 3856–3867.
68. Czech, M. P., M. Tencerova, D. J. Pedersen, and M. Aouadi. 2013. Insulin signalling mechanisms for triacylglycerol storage. *Diabetologia.* **56:** 949–964.
69. Zabielski, P., A. Blachnio-Zabielska, I. R. Lanza, S. Gopala, S. Manjunatha, D. R. Jakaitis, X. M. Persson, J. Gransee, K. A. Klaus, J. M. Schimke, et al. 2014. Impact of insulin deprivation and treatment on sphingolipid distribution in different muscle subcellular compartments of streptozotocin-diabetic C57Bl/6 mice. *Am. J. Physiol. Endocrinol. Metab.* **306:** E529–E542.
70. Nawrocki, A., M. Gorska, B. Wojcik, and A. Buslowska. 1999. Effect of streptozotocin diabetes on fatty acid content and composition of the heart lipids in the rat. *Rocz. Akad. Med. Bialymst.* **44:** 170–179.
71. Pighin, D., L. Karabatas, C. Pastorale, E. Dascal, C. Carbone, A. Chicco, Y. B. Lombardo, and J. C. Basabe. 2005. Role of lipids in the early developmental stages of experimental immune diabetes induced by multiple low-dose streptozotocin. *J. Appl. Physiol.* **98:** 1064–1069.
72. Błachnio-Zabielska, A., P. Zabielski, M. Baranowski, and J. Gorski. 2010. Effects of streptozotocin-induced diabetes and elevation of plasma FFA on ceramide metabolism in rat skeletal muscle. *Horm. Metab. Res.* **42:** 1–7.
73. Luiken, J. J., Y. Arumugam, R. C. Bell, J. Calles-Escandon, N. N. Tandon, J. F. Glatz, and A. Bonen. 2002. Changes in fatty acid transport and transporters are related to the severity of insulin deficiency. *Am. J. Physiol. Endocrinol. Metab.* **283:** E612–E621.
74. Ishibashi, Y., and Y. Hirabayashi. 2015. AMP-activated protein kinase suppresses biosynthesis of glucosylceramide by reducing intracellular sugar nucleotides. *J. Biol. Chem.* **290:** 18245–18260.
75. Xu, X., S. Kobayashi, K. Chen, D. Timm, P. Volden, Y. Huang, J. Gulick, Z. Yue, J. Robbins, P. N. Epstein, et al. 2013. Diminished autophagy limits cardiac injury in mouse models of type 1 diabetes. *J. Biol. Chem.* **288:** 18077–18092.
76. Bugger, H., and E. D. Abel. 2009. Rodent models of diabetic cardiomyopathy. *Dis. Model. Mech.* **2:** 454–466.
77. Funai, K., H. Song, L. Yin, I. J. Lodhi, X. Wei, J. Yoshino, T. Coleman, and C. F. Semenkovich. 2013. Muscle lipogenesis balances insulin sensitivity and strength through calcium signaling. *J. Clin. Invest.* **123:** 1229–1240.
78. Taddeo, E. P., R. C. Laker, D. S. Breen, Y. N. Akhtar, B. M. Kenwood, J. A. Liao, M. Zhang, D. J. Fazakerley, J. L. Tomsig, T. E. Harris, et al. 2014. Opening of the mitochondrial permeability transition pore links mitochondrial dysfunction to insulin resistance in skeletal muscle. *Mol. Metab.* **3:** 124–134.
79. Baranowski, M., A. Blachnio-Zabielska, T. Hirnle, D. Harasiuk, K. Matlak, M. Knapp, P. Zabielski, and J. Gorski. 2010. Myocardium of type 2 diabetic and obese patients is characterized by alterations in sphingolipid metabolic enzymes but not by accumulation of ceramide. *J. Lipid Res.* **51:** 74–80.
80. Baranowski, M., and J. Gorski. 2011. Heart sphingolipids in health and disease. *Adv. Exp. Med. Biol.* **721:** 41–56.
81. Fox, T. E., X. Han, S. Kelly, A. H. Merrill 2nd, R. E. Martin, R. E. Anderson, T. W. Gardner, and M. Kester. 2006. Diabetes alters sphingolipid metabolism in the retina: a potential mechanism of cell death in diabetic retinopathy. *Diabetes.* **55:** 3573–3580.
82. Zador, I. Z., G. D. Deshmukh, R. Kunkel, K. Johnson, N. S. Radin, and J. A. Shayman. 1993. A role for glycosphingolipid accumulation in the renal hypertrophy of streptozotocin-induced diabetes mellitus. *J. Clin. Invest.* **91:** 797–803.
83. Yabu, T., A. Shimuzu, and M. Yamashita. 2009. A novel mitochondrial sphingomyelinase in zebrafish cells. *J. Biol. Chem.* **284:** 20349–20363.
84. Bionda, C., J. Portoukalian, D. Schmitt, C. Rodriguez-Lafrasse, and D. Ardail. 2004. Subcellular compartmentalization of ceramide metabolism: MAM (mitochondria-associated membrane) and/or mitochondria? *Biochem. J.* **382:** 527–533.
85. Ezanno, H., J. le Bloc'h, E. Beauchamp, D. Lagadic-Gossmann, P. Legrand, and V. Rioux. 2012. Myristic acid increases dihydroceramide Δ4-desaturase 1 (DES1) activity in cultured rat hepatocytes. *Lipids.* **47:** 117–128.
86. Fujimoto, M., and T. Hayashi. 2011. New insights into the role of mitochondria-associated endoplasmic reticulum membrane. *Int. Rev. Cell Mol. Biol.* **292:** 73–117.
87. Helle, S. C., G. Kanfer, K. Kolar, A. Lang, A. H. Michel, and B. Kornmann. 2013. Organization and function of membrane contact sites. *Biochim. Biophys. Acta.* **1833:** 2526–2541.
88. Vance, J. E. 2014. MAM (mitochondria-associated membranes) in mammalian cells: lipids and beyond. *Biochim. Biophys. Acta.* **1841:** 595–609.
89. Ardail, D., I. Popa, J. Bodennec, P. Louisot, D. Schmitt, and J. Portoukalian. 2003. The mitochondria-associated endoplasmic-reticulum subcompartment (MAM fraction) of rat liver contains highly active sphingolipid-specific glycosyltransferases. *Biochem. J.* **371:** 1013–1019.
90. Andreyev, A. Y., Y. E. Kushnareva, and A. A. Starkov. 2005. Mitochondrial metabolism of reactive oxygen species. *Biochemistry (Mosc).* **70:** 200–214.
91. Vazquez, E. J., J. M. Berthiaume, V. Kamath, O. Achike, E. Buchanan, M. M. Montano, M. P. Chandler, M. Miyagi, and M. G. Rosca. 2015. Mitochondrial complex I defect and increased fatty acid oxidation enhance protein lysine acetylation in the diabetic heart. *Cardiovasc. Res.* **107:** 453–465.
92. Bugger, H., D. Chen, C. Riehle, J. Soto, H. A. Theobald, X. X. Hu, B. Ganesan, B. C. Weimer, and E. D. Abel. 2009. Tissue-specific remodeling of the mitochondrial proteome in type 1 diabetic akita mice. *Diabetes.* **58:** 1986–1997.
93. Shen, X., S. Zheng, V. Thongboonkerd, M. Xu, W. M. Pierce, Jr., J. B. Klein, and P. N. Epstein. 2004. Cardiac mitochondrial damage and biogenesis in a chronic model of type 1 diabetes. *Am. J. Physiol. Endocrinol. Metab.* **287:** E896–E905.
94. Yu, R. K., Y. Nakatani, and M. Yanagisawa. 2009. The role of glycosphingolipid metabolism in the developing brain. *J. Lipid Res.* **50(Suppl):** S440–S445.
95. Pastorino, J. G., M. Tafani, R. J. Rothman, A. Marcinkeviciute, J. B. Hoek, J. L. Farber, and A. Marcineviciute. 1999. Functional consequences of the sustained or transient activation by Bax of the mitochondrial permeability transition pore. *J. Biol. Chem.* **274:** 31734–31739. [Erratum. 2000. *J. Biol. Chem.* **275:** 8262.]
96. Hisaki, H., H. Shimasaki, N. Ueta, M. Kubota, M. Nakane, T. Nakagomi, A. Tamura, and H. Masuda. 2004. In vivo influence of ceramide accumulation induced by treatment with a glucosylceramide synthase inhibitor on ischemic neuronal cell death. *Brain Res.* **1018:** 73–77.